A Two-Component System that Modulates Cyclic-di-GMP Metabolism Promotes *Legionella pneumophila* Differentiation and Viability in Low-Nutrient Conditions

Elisa D. Hughes, Brenda G. Byrne, Michele S. Swanson[#]

Department of Microbiology and Immunology, University of Michigan Medical School, Ann Arbor, Michigan, USA

[#]Address correspondence to Michele Swanson, PhD; mswanson@umich.edu

ABSTRACT

During its life cycle, the environmental pathogen *Legionella pneumophila* alternates between a replicative and a transmissive cell type when cultured in broth, macrophages, or amoebae. Within a protozoan host, *L. pneumophila* further differentiates into the hardy cell type known as the Mature Infectious Form (MIF). The second messenger cyclic-di-GMP coordinates lifestyle changes in many bacterial species, but its role in the *L. pneumophila* life cycle is less understood. Using an *in vitro* broth culture model that approximates the intracellular transition from the replicative to transmissive form, here we investigate the contribution to *L. pneumophila* differentiation of a two-component system (TCS) that regulates cyclic-di-GMP metabolism. The TCS is encoded by *lpg0278-lpg0277* and is co-transcribed with *lpg0279*, which encodes a protein upregulated in MIF cells. Using a *gfp*-reporter, we demonstrate that the promoter for this operon is RpoS-dependent and induced in nutrient-limiting conditions that do not support replication. The response regulator of the TCS (Lpg0277) is a bifunctional enzyme that both synthesizes and degrades cyclic-di-GMP. Using a panel of site-directed point mutants, we show that cyclic-di-GMP synthesis mediated by a conserved GGDEF domain promotes growth arrest of replicative *L. pneumophila*, production of pigment and poly-3-hydroxybutyrate storage granules, and viability in nutrient-limiting conditions. Genetic epistasis tests predict that the MIF protein Lpg0279 acts upstream of the TCS as a negative regulator. Thus, *L. pneumophila* is equipped with a regulatory network in which cyclic-di-GMP stimulates the switch from a replicative to a resilient state equipped to survive in low-nutrient environments.

IMPORTANCE

Although an intracellular pathogen, *L. pneumophila* has developed mechanisms to ensure long-term survival in low-nutrient aqueous conditions. Eradication of *L. pneumophila* from contaminated water supplies has proven challenging, as outbreaks have been traced to previously remediated systems. Understanding the genetic determinants that support *L. pneumophila* persistence in low-nutrient environments can inform design of remediation methods. Here we characterize a genetic locus that encodes a two-component signaling system (*lpg0278-lpg0277*) and a putative regulator protein (*lpg0279*) that modulates production of the messenger molecule cyclic-di-GMP. We show that this locus promotes both *L. pneumophila* cell differentiation and survival in nutrient-limiting conditions, thus advancing our understanding of the mechanisms that contribute to *L. pneumophila* environmental resilience.

INTRODUCTION

Legionella pneumophila is a gram-negative bacterium commonly found in aquatic environments, where it replicates within protozoan hosts and persists within biofilms (1). When inhaled, contaminated water droplets transmit *L. pneumophila* to the human lung, where this opportunistic pathogen can infect alveolar macrophages. Studies examining the life cycle of *L. pneumophila* cultured in broth, macrophages, and amoebae support a developmental model in which nutrient levels govern cellular differentiation (2, 3). When nutrients are plentiful, the bacteria activate pathways that support growth; when nutrients become limiting, the progeny stop replicating and express multiple factors that promote *L. pneumophila* transmission to a new host, including flagella and the Dot/Icm Type IV secretion system (4). Within protozoan hosts, *L. pneumophila* can differentiate further to generate the resilient, metabolically dormant but highly

55 infectious Mature Infectious Form (MIF), a cell-type believed to be prevalent in the environment
56 (5, 6).

57 To alternate between replication within phagocytes and persistence within nutrient-poor
58 aquatic environments, *L. pneumophila* relies on multiple regulatory mechanisms that coordinate
59 rapid adaption to changing conditions (3). For example, replication in broth requires amino acids
60 as the primary carbon source (7, 8), and a reduction in amino acid availability activates
61 regulatory pathways that trigger conversion from the exponential (E) phase to the post-
62 exponential (PE) transmissive phase (9, 10). The *L. pneumophila* life cycle is governed by a
63 sophisticated regulatory network that includes the stringent response enzymes RelA and SpoT,
64 multiple alternative sigma factors including RpoS and FliA, two-component regulatory systems,
65 small regulatory RNAs, and CsrA post-transcriptional repressors (3, 11, 12). Driving the E to PE
66 differentiation is a stringent response pathway coordinated by the alarmone guanosine penta- and
67 tetraphosphate (abbreviated here as ppGpp) (13). The two-component system LetA/LetS
68 responds to ppGpp accumulation by inducing transcription of small regulatory RNAs RsmY and
69 RsmZ (14-16). These non-coding RNAs bind to and relieve repression by CsrA, enabling
70 expression of multiple virulence traits associated with PE phase *L. pneumophila* including
71 cytotoxicity, motility, and lysosome evasion (reviewed by 3).

72 Another second messenger molecule that regulates lifestyle switches in *L. pneumophila*
73 and multiple other bacterial species is bis-(3'-5')-cyclic dimeric guanosine (c-di-GMP) (4-8).
74 Diguanylate cyclases (DCG), which possess a conserved GGDEF motif, synthesize c-di-GMP
75 from two molecules of GTP. Conversely, phosphodiesterases (PDE) catalyze the hydrolysis of c-
76 di-GMP back to GMP and contain either an EAL or HD-GYP domain (17). Most bacterial
77 species utilizing c-di-GMP produce multiple enzymes that control c-di-GMP levels; for example,

Escherichia coli encodes 29 proteins with GGDEF and/or EAL domains (18), and *Vibrio cholera* encodes over 60 such proteins (19).

The *L. pneumophila* genome (Philadelphia-1 and Lens strains) encodes 22 different enzymes involved in c-di-GMP metabolism, including several composite proteins possessing both GGDEF and EAL domains (20, 21). The range of activities influenced by these proteins is diverse and even includes control of opposing biological functions within the same cell. Recently Pecastings *et al*. (22) identified five c-di-GMP proteins in the Lens strain involved in biofilm regulation, three of which enhance biofilm formation while the other two inhibit this developmental program. In *L. pneumophila*, some c-di-GMP producing and degrading proteins enhance virulence by altering translocation of multiple Dot/Icm Type IV secretion system effectors, interfering with phagosome/lysosome fusion, and enhancing cytotoxicity—functions that promote replication within and transmission between host cells (20, 21). In general, GGDEF and/or EAL motifs are crucial for the protein's enzymatic activity (21). However, genetic disruption of these domains does not always cause detectable changes in the cellular c-di-GMP concentration, leaving open the possibility that some of these proteins perform regulatory roles independently of c-di-GMP metabolism (20, 22).

Two-component regulatory systems, classically comprised of a histidine kinase and a response regulator, are a widespread signal transduction mechanism in bacteria that enables rapid adaptation to fluctuating conditions (reviewed by 23, 24). Some response regulators contain GGDEF and/or EAL domains; when phosphorylated on a conserved aspartate residue by its cognate histidine kinase, these enzymes can alter their c-di-GMP synthesis or hydrolysis (25). For example, in *Xanthomonas campestris*, the composite GGDEF/EAL protein RavR is the response regulator in a two-component system whose activation by the histidine kinase RavA

shifts the enzyme from DCG to PDE activity and ultimately increases virulence (26). In the *L. pneumophila* Lens strain, Levet-Paulo et al. (27) characterized a putative two-component system comprised of a histidine kinase Lp0330 and its cognate response regulator Lpl0329, a bifunctional enzyme with both a GGDEF and an EAL domain. A series of *in vitro* experiments using purified proteins demonstrated that Lpl0329 possesses both DGC and the opposing PDE enzymatic activity, and phosphotransfer from Lpl0330 to Lpl0329 reduces DGC activity (27). In the *L. pneumophila* Philadelphila-1 strain, the homolog of Lpl0330 is Lpg0278 (hereafter HK), and the homolog of Lpl0329 is Lpg0277 (hereafter RR; HK and RR collectively are hereafter the TCS). On the Philadelphia-1 chromosome located directly 5' of *lpg0278* and *lpg0277* is *lpg0279*, a gene encoding a hypothetical protein that is abundant in MIF cells (6).

The genetic proximity of the MIF gene *lpg0279* to the TCS-encoding *lpg0277* and *lpg0278* loci suggest potential co-regulation and related functions (28). As MIF cells are resilient forms that develop from PE phase *L. pneumophila* within protozoan hosts (10), here we test the hypothesis that the locus consisting of *lpg0279*, *lpg0278* and *lpg0277* (hereafter referred to as *lpg0279-77*) promotes persistence of *L. pneumophila* in nutrient-poor environments.

RESULTS

lpg0277, *lpg0278* and *lpg0279* are co-transcribed

The TCS-encoding genes *lpg0277* and *lpg0278* are located on the same DNA strand, 22 bp 3' of *lpg0279*. To test the hypothesis that these three genes constitute an operon, we analyzed RNA extracted from wild-type (WT) *L. pneumophila* cultured to PE phase in rich AYET media. After conversion to cDNA, an endpoint PCR assay was conducted using primer sets designed to span the intergenic regions between the three genes (Fig. 1A). As predicted, amplicons of ~300 bp

were generated by primer sets A/B as well as by primers C/D, indicating that *lpg0279* and *lpg0278* form a single transcriptional unit, as do *lpg0278* and *lpg0277* (Fig. 1B). A similar experiment was conducted to determine if this transcriptional unit includes *lpg0280*, which is located 165 bp 5' of *lpg0279* and codes for a putative transcriptional regulator of the LysR family. No product was generated for primer pairs E/F (Fig 1C), indicating that the operon consists solely of *lpg0279*, *lpg0278* and *lpg0277.*

The *lpg0279-77 locus* is induced at the transition from E to PE phase

To begin to delineate the role of *lpg0279-77* in the *L. pneumophila* life cycle, we first analyzed the timing and conditions that induce its promoter activity. To do so, we generated a transcriptional reporter by ligating a DNA fragment corresponding to the 832 bp immediately 5' of the *lpg0279* open reading frame to a promoterless copy of the *gfp-mut3* gene encoded on plasmid pBH6119 (29), generating p*lpg0279-gfp.* This transcriptional reporter was then transferred to WT *L. pneumophila*.

Expression of *lpg0279-gfp* was monitored in E and PE phase broth cultures, which function as proxies for the intracellular replicative and transmissive stages, respectively (2, 4). In each case, E phase cultures were sub-cultured to an OD_{600} of 0.4-0.8 in rich AYE media, incubated at 37°C on an orbital shaker, and then GFP fluorescence and cell density were measured at 2-3 h intervals. As a reference for PE phase expression, a transcriptional reporter strain in which *gfp* expression is driven by the promoter for the flagellin subunit *flaA* (p*flaA-gfp*) was analyzed in parallel (13). Serving as the negative control was a strain carrying the promoterless *gfp* vector pBH6119. All strains grew equally well as measured by OD_{600}, and no fluorescence was observed for the vector control (Fig. 2). Throughout E phase, the p*lpg0279-gfp*

147 strain generated only minimal levels of GFP fluorescence, whereas promoter activity increased
148 markedly upon entry into PE phase—kinetics similar to that of the p*flaA-gfp* marker of the PE
149 transmissive phase (Fig. 2).
150
151 **The stationary phase sigma factor RpoS activates *lpg0279-77* expression**
152 Due to the temporal similarity of their promoter activation (Fig. 2), we postulated that
153 transcription of *lpg0279-77* and *flaA* may be controlled by the same regulatory proteins.
154 Therefore, we assessed the contribution of a subset of the regulators known to coordinate the *L.*
155 *pneumophila* transition from E to PE phase (16, 30-33). To do this, the p*lpg0279-gfp* and p*flaA-*
156 *gfp* reporters were transformed into mutants lacking either the alternative sigma factors FliA (σ^{28})
157 or RpoS (σ^{S}/σ^{38}), the two-component system LetA/S, or the ppGpp synthetase RelA. This panel
158 of strains was then cultured on CYET agar at 37°C for 3 days. Visible differences in GFP
159 expression indicated that RpoS is essential for robust transcription of *lpg0279-77*, but the other
160 regulatory factors were not (Fig. 3A). In contrast, p*flaA-gfp* expression was only marginally
161 diminished in the *rpoS* mutant; as expected, the FliA sigma factor was its critical regulator (Fig.
162 3B) (32, 34). Thus, although the promoters for *flaA* and *lpg0279-77* are each induced in PE
163 phase, their mechanisms of regulation differ; accordingly, these two loci may respond to distinct
164 environmental signals.
165
166 **Expression of *lpg0279-77* increases in the absence of amino acids essential for replication**
167 First identified in *E. coli* (35), the stationary phase sigma factor RpoS is widespread in
168 proteobacteria (36). RpoS is a key regulator of the stringent response, which facilitates bacterial
169 adaptation to a range of stresses, including starvation (37). When nutrients become limiting,

replicating *L. pneumophila* accumulate the alarmone ppGpp and synthesize RpoS, which activates expression of multiple genes critical for fitness in the PE phase (3).

Because *lpg0279-77* transcription is RpoS-dependent, we next examined whether *lpg0279-gfp* expression by replicating bacteria was induced when nutrients were limited. Standard growth media for *L. pneumophila* consists of a rich media (AYE) supplemented with both iron and the amino acid L-cysteine, as this bacterium lacks a number of cysteine biosynthesis enzymes (38, 39). Accordingly, we first quantified *lpg0279-gfp* fluorescence in *L. pneumophila* cultured in AYE containing both L-cysteine and ferric nitrate, either L-cysteine or ferric nitrate alone, or neither supplement. In media supplemented with L-cysteine, either with or without additional iron, *L. pneumophila* continued to replicate for > 9 hours and did not activate the *lpg0279-77* promoter (Fig. 4A). In contrast, when cultures lacked L-cysteine, bacterial replication stalled and the *lpg0279-77* promoter was induced (Fig. 4A).

The yeast extract in AYE contains several amino acids including L-cysteine (bdbiosciences.com), so to more accurately address the impact of this amino acid in promoting *lpg0279-77* expression we repeated the analysis using a chemically defined medium (CDM) (38) in which L-cysteine, L-cystine, and supplemental ferric pyrophosphate were omitted. Initial experiments examined *lpg0279-gfp* fluorescence in CDM containing a range of L-cysteine concentrations: 100% (2.27 mM), 50% (1.14 mM) and 25% (0.57 mM) of the standard concentration used to support *in vitro* growth in rich AYE media. In each case, the presence of L-cysteine repressed expression of *lpg0279-gfp* by replicating *L. pneumophila* (Fig. 4B).

These experiments also revealed an inverse relationship between *lpg0279-77* promoter activity and bacterial growth (Figs. 4A-B; also see Fig. 2). Specifically, the absence of L-cysteine hindered bacterial replication and induced *lpg0279-77* gene expression. One

193 interpretation is that *lpg0279-77* transcription is triggered by the absence of this particular amino
194 acid; in turn, the locus suppresses replication. Alternatively, the inability of *L. pneumophila* to
195 replicate in the absence of an essential amino acid—in this case L-cysteine—may be a signal that
196 induces *lpg0279-77* expression. To distinguish between these two possibilities, we examined
197 *lpg0279-gfp* fluorescence in CDM lacking either L-serine or L-methionine, two amino acids *L.*
198 *pneumophila* requires for growth in CDM (38). Compared to cultures in complete CDM, lack of
199 either L-serine or L-methionine reduced replication and enhanced p*lpg0279-gfp* expression (Fig.
200 4C). Thus, *L. pneumophila* induces *lpg0279-77* promoter activity in response to nutrient-limiting
201 conditions that impede bacterial replication.
202
203 **PE phase *L. pneumophila* lacking either the HK or RR component of the TCS, or**
204 **constitutively expressing *lpg0279*, exhibit a shortened lag phase and reduced pigmentation**
205 Based on the increase in *lpg0279-77* promoter activity observed in response to conditions
206 that do not support *L. pneumophila* growth (Figs. 2 and 4), we next examined whether this locus
207 influences differentiation of replicating *L. pneumophila* to the PE phase. To do so, we generated
208 isogenic mutants containing in-frame deletions in either *lpg0279*, *lpg0278*, or *lpg0277*.
209 To assess growth of each mutant strain, overnight E phase (OD_{600} < 2.5) or PE phase
210 (OD_{600} < 3.5) cultures were diluted to an OD_{600} of 0.1 in AYET, and then cell density was
211 quantified over a 36 h period using a Bioscreen growth curve analyzer. For the E phase inocula,
212 growth curves for each mutant resembled the WT strain (data not shown). However, for the PE
213 phase inocula, mutants lacking either the HK (Δ*lpg0278*) or RR (Δ*lpg0277*) component of the
214 TCS mimicked the WT E phase reference culture by exhibiting a minimal lag phase (Fig. 5A and
215 B). Although expression of each individual WT gene from an IPTG-inducible promoter was

insufficient to remedy this defect (data not shown), IPTG-induced expression of the *lpg0278-lpg0277* locus from plasmid pHK/RR restored WT growth kinetics (Fig. 5A and B).

In contrast to the TCS genes, growth of mutants lacking *lpg0279* was indistinguishable from WT PE phase cultures (Fig. 5C). However, WT *L. pneumophila* constitutively expressing a plasmid-borne allele of *lpg0279* engineered to encode an optimal ribosome binding site (20) exhibited growth kinetics similar to the ΔHK or ΔRR mutants and E phase WT *L. pneumophila* (Fig. 5C). Therefore, constitutive expression of *lpg0279* inhibits replicating *L. pneumophila* from transitioning to PE phase, whereas the genetically-linked TCS promotes differentiation of replicating *L. pneumophila* to the PE phase.

To test more rigorously the impact of the TCS and Lpg0279 on *L. pneumophila* differentiation, we quantified production of the soluble pigment pyomelanin, a late PE phase trait (40, 41). Derived from secreted homogentisic acid (HGA), this melanin-like substance is not required for intracellular survival; rather it enhances environmental fitness of *L. pneumophila* by protecting bacterial cells from the damaging effects of light and by aiding in iron acquisition through its ferric reductase activity (42, 43). When cultured in rich broth to a cell density typical of PE phase (OD_{600} > 3.5), all strains generated minimal pigment. However, when maintained in PE phase for up to three days, WT cultures accumulated pigment, but strains that lacked either of the TCS components did not (Fig. 5D). Consistent with their growth phenotypes, deletion of the *lpg0279* gene had no effect, whereas constitutive expression of *lpg0279* by WT *L. pneumophila* inhibited pigment accumulation (Fig. 5D). Consistently, the ΔRR mutant harboring the complementing plasmid pHK/RR produced higher levels of pigment than did the WT strain, indicating that the TCS in multi-copy may stimulate differentiation to PE phase. As TCS integrity appears essential for the transition from E to PE phase in *L. pneumophila*, we next

239 examined whether the TCS enhances *L. pneumophila* viability when nutrients are limiting. In
240 TCS signal transduction pathways, RR activity is distal to HK; accordingly, we analyzed the RR
241 mutant as representative of Lpg0278-0277 TCS output.
242
243 **The TCS facilitates PHB production and long-term survival in low-nutrient conditions**
244 Beginning in the PE phase, *L. pneumophila* generates large poly-3-hydroxybutyrate (PHB)
245 inclusions, a reserve carbon and energy source that accumulates in MIF cells (5, 44) and
246 enhances persistence of *L. pneumophila* in low-nutrient environments (45). Therefore, we next
247 quantified the PHB content of WT and the ΔRR mutant using the lipophilic dye Nile Red, a
248 fluorescent stain that is highly specific for intracellular lipids, including PHB (46). To determine
249 the baseline value, the fluorescence of E phase cultures in AYET was quantified. Next, after
250 collecting WT and ΔRR mutant cells by centrifugation, their expression of *lpg0279-77* was
251 induced by resuspending each cell sample in CDM media lacking L-cysteine (Fig. 4B), and then
252 the bacteria were incubated for 24 h at 37°C with aeration before a second PHB quantification.
253 As expected, in E phase the Nile Red PHB signal for both WT and ΔRR was negligible.
254 However, after 24 h of nutrient limitation, the WT cells exhibited significantly greater
255 fluorescence than did the ΔRR mutant (Fig. 6A). Expression by the mutant of the TCS from
256 pHK/RR not only fully remedied this defect, but also generated a PHB signal exceeding that of
257 the WT strain. Therefore, the TCS promotes accumulation of PHB storage granules in *L.*
258 *pneumophila*.
259 As this TCS equips replicating *L. pneumophila* to respond to nutrient limitation by
260 transitioning to the PE phase, producing pigment, and accumulating PHB storage granules—all
261 traits that increase resilience in the environment—we next investigated whether this TCS

facilitates *L. pneumophila* survival during prolonged exposure to low-nutrient conditions. To do so, we quantified CFUs of WT and ΔRR mutant cells first in E phase and then again after 3 and 7 d incubation in CDM lacking L-cysteine, as described for the Nile Red fluorescence experiments. Indeed, compared to WT, the ΔRR strain suffered a greater loss of viability by day 7, a defect remedied by ectopic expression of the TCS locus (Fig. 6B). Therefore, *L. pneumophila* persistence in nutrient-limited conditions is enhanced by the *lpg0277* locus, which encodes an enzyme equipped to modulate levels of the second messenger c-di-GMP.

The GGDEF domain of Lpg0277 promotes transition from E to PE phase

Because the RR is a bifunctional enzyme with both DGC and PDE activity (27), we next examined which of these opposing functions accounts for the ΔRR mutant phenotypes. To do so, we took advantage of the known contributions of the GGDEF and EAL amino acid motifs to DCG and PDE activity, respectively (17, 25). To abrogate DGC function, we engineered point mutant strains in which the conserved Glu-396 residue was replaced with Lys (27), generating the RR^{E396K} allele. Likewise, to impair PDE activity, the Glu-521 residue in the EAL domain was replaced with Ala, creating the RR^{E521A} allele (18). After confirming the DNA sequence of each *L. pneumophila* chromosomal point mutation, the corresponding mutant strains were transformed with either the complementing plasmid pHK/RR or the empty vector.

We first examined the growth kinetics and pigment production of the RR^{E396K} DCG and RR^{E521A} PDE point mutants after culturing to an $OD_{600} > 3.5$, correlating with PE phase in WT cells. The RR^{E521A} PDE mutant mimicked PE phase WT cells in growth kinetics (Fig. 7B), and its pigment production exceeded that of the WT strain (Fig. 7C). In contrast, the RR^{E396K} DCG mutant resembled E phase WT cells, as judged by its minimal lag phase (Fig. 7A) and decreased

285 pigmentation (Fig. 7C), two defects that were complemented by ectopic expression of the WT
286 TCS. Thus, the GGDEF motif of the RR promotes the transition of replicating *L. pneumophila* to
287 the PE phase.

288 To further probe RR function, we genetically abrogated the ability of the RR to be
289 phosphorylated by its cognate HK, a post-translational modification that induces a change in RR
290 enzymatic activity (27). For this purpose, the conserved Asp-87 residue in the putative
291 phosphoacceptor site of the RR was replaced with Asn, generating mutant strain RR^{D87N} (27).
292 The RR^{D87N} phosphoacceptor mutant exhibited growth and pigmentation defects similar to that
293 observed for both the ΔRR and RR^{E396K} DGC mutants (Fig. S1; also Figs. 5 & 7), indicating a
294 functional link between TCS phosphorylation and RR DGC activity.

295 Based on our growth and pigmentation analyses, we investigated whether abrogated DGC
296 activity accounted for the reduction in both PHB levels and viability of ΔRR mutant cells (Fig. 6).
297 To test this hypothesis, we exposed E phase cultures of the RR^{E396K} DGC, RR^{E521A} PDE, and
298 RR^{D87N} phosphoacceptor point mutants to CDM lacking L-cysteine, and then quantified PHB
299 production via Nile Red florescence and survival via CFU enumeration, as described for the
300 ΔRR mutant analysis (Fig. 6). As expected, PHB accumulation by the RR^{E521A} PDE mutant was
301 indistinguishable from WT *L. pneumophila*, and both strains survived well after 7 d exposure to
302 CDM lacking L-cysteine (Fig. S2A). However, the RR^{E396K} DCG and RR^{D87N} phosphoacceptor
303 point mutants each had reduced PHB content, as judged by Nile Red fluorescence (Figs. S2B-C).
304 Both strains also lost viability after extended CDM exposure, a phenotype mimicking the ΔRR
305 strain (Fig. S2B-C and 6B). It is notable that these defects were only partially complemented,
306 perhaps due to unknown effects of perturbed cellular c-di-GMP pools. Nevertheless, the
307 phenotypic profile of each point mutant is consistent with a model in which DCG activity and

concomitant accumulation of cyclic-di-GMP stimulates replicating *L. pneumophila* to transition to PE phase and generate PHB stores that support bacterial survival in nutrient-limited conditions.

Ectopic expression of *lpg0279* counteracts TCS function

The spatial proximity and co-regulation of *lpg0279* with the TCS-encoding genes *lpg0277* and *lpg0278* (Fig. 1) suggest a regulatory interaction. Since WT cells constitutively expressing *lpg0279* phenocopy the growth and pigmentation defects of the ΔRR and RR^{E396K} DCG mutants (Figs. 5 & 7), we hypothesized that Lpg0279 functions as a negative regulator of TCS activity.

To investigate whether Lpg0279 acts upstream of the TCS, the RR^{E521A} PDE point mutant—which resembles WT in the transition from E to PE phase (Fig. 7B-C)—was transformed with plasmid p*lpg0279* and then treated with IPTG to induce constitutive expression. In parallel, we also transformed the RR^{E396K} mutant with p*lpg0279* to evaluate any additive effects of loss of DGC activity and gain of Lpg0279 function. After culturing both strains to an $OD_{600} > 3.5$, we performed growth curve and pigmentation analyses. As expected, expression of *lpg0279* did not rescue the growth defect of the RR^{E396K} DCG mutant strain (Fig. S3A). However, *lpg0279* expression significantly shortened the lag phase of the RR^{E521A} PDE mutant to that of WT E phase cells (Fig. S3B). Assessment of pigment production yielded similar results, with *lpg0279* expression reducing pigment levels in the RR^{E521A} mutant but having no effect on the RR^{E396K} mutant cells (Fig. 8A). Furthermore, when exposed to CDM lacking L-cysteine for 7 d, both the WT and RR^{E521A} PDE mutant strains harboring p*lpg0279* suffered a significant drop in cell viability compared to the respective parent strains (Fig. 8B). These data indicate that *lpg0279* is epistatic to the TCS genes, acting as a negative regulator. In low-nutrient conditions,

and in the presence or absence of an inducing signal, repression by Lpg0279 is relieved, enhancing DCG activity of the RR and increasing c-di-GMP. Although the downstream effectors of c-di-GMP generated by the RR remain to be identified, the activity of this TCS stimulate *L. pneumophila* to switch from a replicative state to a more resilient cell type better equipped to survive in low-nutrient environments.

DISCUSSION

As an intracellular pathogen, *L. pneumophila* has evolved multiple mechanisms to survive and replicate in a wide variety of environments, ranging from freshwater protozoans and human lung macrophages to nutrient-poor natural or engineered water systems. To thrive in such diverse conditions, *L. pneumophila* responds to environmental stimuli by alternating between distinct cell types. Amino acid or fatty acid starvation triggers replicating *L. pneumophila* to transition to a highly motile and infectious transmissive form, and prolonged starvation stimulates further development to the hardy MIF cell type (5, 10, 13, 47). Using an *in vitro* culture model to analyze the switch between replicative, transmissive, and resilient cell types, here we identify as a regulatory component an operon designed to regulate cyclic-di-GMP metabolism. This operon consists of *lpg0279*, which codes for a protein abundant in MIF cells (6), and *lpg0278-lpg0277*, which encodes a two-component system (TCS) (27). Together, Lpg0279 and the TCS equip *L. pneumophila* to respond to nutrient deprivation by differentiating to a non-replicative cell type that generates pigment, accumulates PHB storage granules, and maintains viability.

The *lpg0279-77* operon is induced by the stationary phase sigma factor RpoS in response to nutrient limitation (Figs. 1-4). Indeed, to survive prolonged amino acid limitation, *L.*

354 *pneumophila* require not only a functional TCS (Fig. 6B) but also RpoS (48). Thus, RpoS equips
355 *L. pneumophila* to express factors that enhance resilience in nutrient-poor environments, in part
356 by promoting TCS-mediated production of c-di-GMP (Figs. 3 and 6) (48-51).
357 One factor that promotes persistence of environmental *L. pneumophila* is secretion of the
358 pigment pyomelanin, which occurs in late PE phase. Derived from polymerization of
359 homogentisic acid (HGA), this soluble pigment not only protects *L. pneumophila* from the
360 damaging effects of light (42), but it also possesses ferric reductase activity that contributes to
361 iron uptake (43). A second factor that increases environmental persistence of *L. pneumophila* is
362 poly-3-hydroxybutyrate (PHB). To generate a reserve energy source, *L. pneumophila* increases
363 production of PHB lipid granules at the transition to PE phase (44, 45). Formation of this energy
364 store involves multiple enzymatic steps, and *L. pneumophila* encodes multiple PHB biosynthesis
365 genes. The Lpg0278/Lpg0277 TCS equips *L. pneumophila* to respond to nutrient deprivation by
366 supporting robust PHB accumulation (Fig. 6A); however, additional regulators likely contribute
367 to the process, since *L. pneumophila* that lack the RR still generate some PHB, as judged by Nile
368 Red fluorescence (Fig. 6). Future studies can identify the mechanism of TCS-mediated activation
369 of PHB biosynthesis and the downstream effector of RR-generated c-di-GMP. Candidates for
370 the TCS regulon include *L. pneumophila* genes induced in response to nutrient-limiting
371 conditions (52).
372 A second messenger molecule, c-di-GMP is a wide-spread regulator of multiple bacterial
373 physiological processes, including biofilm formation, cell cycle progression, and virulence gene
374 expression (25, 53-55). The RR encoded by *lpg0277* is a bifunctional enzyme whose DCG and
375 PDE domains can generate and degrade c-di-GMP production, respectively (20). When *L.*
376 *pneumophila* Philadelphila-1 cells experience nutrient deprivation, activation of the TCS is

377 predicted to increase c-di-GMP levels, based on several genetic tests of RR function. In
378 particular, point mutations in either the RR DGC domain (Figs. 7A and C, S2B) or
379 phosphoacceptor site (Figs. S1, S2C) phenocopy the ΔRR mutant (Figs. 5B and D, 6), whereas
380 the PDE domain point mutant resembles WT (Figs. 7B and C, S2A). Our observations are
381 consistent with the studies by Pecastings and colleagues of this locus in the *L. pneumophila* Lens
382 strain: after 5 days culture on solid bacteriology medium, mutants lacking the homologous RR
383 Lpl0329 contain less intracellular c-di-GMP than do WT cells (22). Thus, in non-replicating *L.*
384 *pneumophila* cells, the DCG activity of RR Lpl0329 likely predominates. On the other hand,
385 using proteins purified from the *L. pneumophila* Lens strain, Levet-Paulo and colleagues
386 demonstrated that phosphorylation of the RR Lpl0329 reduced its DCG activity but left PDE
387 activity unaltered (27). These biochemical experiments suggest that the TCS phosphorelay can
388 decrease the local c-di-GMP level. Perhaps these differences between the *in vivo* and *in vitro*
389 studies indicate that the enzymatic activity of RR Lpl0329 can be modulated not only through
390 phosphorylation by its cognate HK, but also by another regulatory factor that does not co-purify
391 with the HK or RR proteins.

392 One factor that does functionally interact with the TCS is Lpg0279, a protein that is
393 conserved among *L. pneumophila*, abundant in MIF cells (6), and encoded on the *lpg0279-0277*
394 mRNA (Fig. 1). Consistent with a function in MIF cells, *L. pneumophila* do not require Lpg0279
395 to transition from E to PE phase in broth. However, constitutive expression of *lpg0279* prevents
396 replicating WT *L. pneumophila* from differentiating to the PE transmissive form, as does loss of
397 TCS function (Fig. 5). Moreover, genetic epistasis tests predict that the MIF protein Lpg0279
398 acts upstream of the TCS, repressing its activity by a mechanism not yet known (Fig. 8, S3B).

One clue to Lpg0279 function is its F-box and Intracellular Signal Transduction (FIST) domain, first recognized in 2007 as a component of signaling pathways in diverse prokaryotic and eukaryotic species (56). In *Pseudomonas aeruginosa*, the FIST domain of protein Pa1975 (NosP) senses nitric oxide and inhibits its co-cistronic HK to promote biofilm dispersal (57). In *L. pneumophila,* another nitric oxide sensor, the Haem-Nitric oxide/Oxygen binding protein Hnox1, is genetically and functionally linked to a GGDEF-EAL protein, Lpg1057; together this protein pair regulates biofilm formation (58). By analogy to these two regulators of bacterial differentiation, a model that warrants testing is that Lpg0279 negatively regulates TCS production of c-di-GMP in response to nitric oxide stress.

Considering our genetic data in the context of the current literature, we favor the following working model for the signal transduction pathway encoded by *lpg0279-77* (Fig. 9). When nutrients become scarce, the stationary phase sigma factor RpoS induces transcription of the *lpg0279-77* operon. As replicating *L. pneumophila* begin to transition to the PE transmissive phase, the Lpg0279 protein initially suppresses TCS production of cyclic-di-GMP. Then in response to additional stress, HK phosphorylates the RR thereby stimulating its DCG activity. An accumulation of cellular c-di-GMP promotes further progression into PE phase, production of pigment and PHB, and survival in nutrient-poor conditions.

This study extends the understanding of the regulatory circuit that governs the *L. pneumophila* life cycle. When nutrients become limiting within host cells, the stringent response alarmone ppGpp coordinates differentiation of intracellular *L. pneumophila* to a motile, infectious form equipped for transmission between host cells. The second messenger cyclic-di-GMP promotes *L. pneumophila* differentiation into a cell type equipped for persistence in nutrient poor environments. Defining c-di-GMP regulatory networks is a challenging endeavor,

422 due to the spatial and temporal sequestering of c-di-GMP signaling, as well as the multiple
423 enzymes that contribute to c-di-GMP metabolism in *L. pneumophila* and other bacteria (25).
424 Accordingly, this genetic analysis of the signal transduction system comprised of the Lpg0279
425 MIF protein and the Lpg0278-Lpg0277 TCS can guide future molecular and biochemical studies
426 to delineate how c-di-GMP promotes resilience of environmental *L. pneumophila*.
427

428 **MATERIALS AND METHODS**

429 **Bacterial strains and culture conditions**

430 The bacterial strains utilized in this study are listed in Supplementary Material **Table S1**.
431 Except where indicated, all *L. pneumophila* strains were cultured in ACES (Sigma)-buffered
432 yeast extract broth (pH = 6.9) supplemented with 0.1 mg/ml thymidine, 0.4 mg/ml L-cysteine,
433 and 0.135 mg/ml ferric nitrate (AYET) or on solid medium containing AYET supplemented with
434 15 g/L agar and 2 g/L charcoal (CYET). Chemically defined medium (CDM) was prepared as
435 previously described (38), except that ferric pyrophosphate and either L-cysteine, L-cystine, L-
436 methionine or L-serine were omitted where indicated. Where necessary for plasmid maintenance,
437 media were supplemented with chloramphenicol (5 µg/ml) and/or kanamycin (10 µg/mL). All *E.*
438 *coli* strains were cultured using Luria-Bertani (LB) broth or agar, supplemented where necessary
439 with ampicillin (100 ug/ml), chloramphenicol (25 µg/ml) or kanamycin (25 µg/ml). To induce
440 gene expression from the pMMB206cam plasmid, 250µM isopropyl β-D-1-
441 thiogalactopyranoside (IPTG; Gold Biotechnology) was added to growth media.
442 Bacteria from frozen stocks were struck onto CYET plates every 1-2 weeks and incubated at
443 37°C for ≥ 3 d until colonies developed. For experiments, colonies were inoculated into AYET
444 and cultured overnight at 37°C on an orbital shaker to exponential (E) phase (OD_{600} < 2.5) and

445 then subcultured in AYET for a second overnight incubation until the desired growth stage: E
446 phase or post-exponential (PE) phase (OD_{600} > 3.5).
447
448 **Plasmids and primers**
449 All plasmids and primers utilized in this study are listed in Supplementary Material **Table S2**.
450 Plasmid p*lpg0279-gfp* was constructed by amplifying the 832 bp directly 5' of the *lpg0279* ORF
451 using primers EH21 and EH43, which encode *Bam*HI and *Xba*I restriction sites, respectively.
452 After digestion, the fragment was then ligated into the GFP reporter plasmid pBH6119 5' of a
453 promoterless *gfpmut3* gene (13, 29). Plasmids pHK/RR and p*lpg0279* were constructed by
454 amplifying either a 3.6 kb fragment containing *lpg0278* through *lpg0277* using primers EH69
455 and EH70 or a 1.2 kb fragment containing *lpg0279* using primers 79OE-F and 79OE-R, which
456 each encode *Bam*HI and *Hind*III restriction sites; primer 79OE-F also encodes an optimal
457 ribosome binding site (20). Following restriction enzyme digestion, the fragments were ligated
458 into the IPTG-inducible plasmid pMMB206cam. Correct placement and orientation of the insert
459 was verified by PCR and/or DNA sequencing.
460
461 **Mutant strain construction**
462 The laboratory strain Lp02, a thymidine auxotroph derived from the clinical isolate
463 Philadelphia-1 (59), was utilized as the parent strain for all constructs. Deletion mutants were
464 generated by homologous recombination as previously described (60) using the primers listed in
465 **Table S2**. The genes of interest along with ~700 bp of 3' and 5' flanking DNA were amplified
466 and cloned into the vector pGEM-T Easy (Promega) to create pGEM*lpg0277*, pGEM*lpg0280*,
467 and pGEM*lpg0279*. The kanamycin cassette from pKD4 was amplified using primers comprised

of the oligos PO and P2 along with ~36 bp of DNA sequence homologous to the regions 3' and 5' of the each gene of interest. Following allelic exchange in the *E. coli* λ-red recombinase strain DY330, candidate colonies were screened by PCR and transformed into *E. coli* host strain DH5α. Point mutants RR^{E396K}, RR^{E521A}, and RR^{D87N} were created using the QuikChange XLII Site-Directed Mutagenesis Kit (Agilent) with plasmid pGEM*lpg0277* serving as a template and using primers sets E396K-F/E396K-R, E521A-F/E521A-R, and D87N-F/D87N-R, respectively. The recombinant alleles (*lpg0277::kan*, *lpg0278::kan* and *lpg0279::kan*) and point mutant alleles were amplified by PCR using each relevant primer pair (77del-F/77del-R, 78del-F/78del-R or 79del-F/79del-R) and introduced into Lp02 by natural transformation. Where indicated in **Table S2**, the kanamycin cassette was subsequently excised by Flp recombinase as previously described (61). All mutations were confirmed by DNA sequencing.

Transformation with the plasmids identified in **Table S1** was conducted by electroporating isolated plasmid DNA (Qiagen) into 50 µl competent cells at 1.8 kV, 100 W and 25 µF using 1 mm cuvettes. Cells were then transferred to 950 µL AYET and incubated at 37°C for 1 h on an orbital shaker before plating on selective media. Also constructed were control strains that carry the corresponding pBH6119 or pMMB206cam empty vector.

RNA isolation

To isolate RNA for analysis, 0.5-1.0 ml of bacterial culture at OD_{600} > 3.0 was collected by centrifugation at 12,000 x g. The pellet was resuspended in an equal volume of TRIzol reagent and then purified using the Direct-zol RNA MiniPrep kit (Zymo Research). All RNA preparations were treated with DNase I Amplification Grade or Turbo DNA-free (Invitrogen), and absence of genomic DNA was confirmed by PCR and gel electrophoresis.

491

492 **End-point PCR experiments**

493 To determine whether *lpg0279*, *lpg0278*, and *lpg0277* are co-transcribed, 800 ng of purified
494 RNA was used as a template to generate cDNA with the iScript cDNA Synthesis Kit (Bio-Rad).
495 End-point PCR was then conducted using primer sets EH13/EH14 and EH1/EH2, which span the
496 *lpg0279-lpg0278* and *lpg0278-lpg0277* intragenic regions, respectively. For the end-point PCR
497 experiment examining co-transcription of *lpg0280* and *lpg0279*, cDNA synthesis was coupled
498 with PCR amplification using 800 ng RNA, primer set EH55/56, and the SuperScript III One-
499 Step RT-PCR System with Platinum *Taq* DNA Polymerase (Invitrogen). For all experiments,
500 genomic DNA was used as a positive control, and reactions omitting the reverse transcriptase
501 enzyme served as a negative control.

502

503 **Growth curves**

504 Bacterial growth kinetics were analyzed by culturing *L. pneumophila* to E or PE phase as
505 indicated, then collecting 1 ml aliquots by centrifugation at 5,000 x g for 5 minutes. The pellet
506 was resuspended to an OD_{600} of 0.1 in 1 ml fresh AYET supplemented with chloramphenicol and
507 ITPG, and 250 µl aliquots were dispensed into triplicate wells of a sterile 100x Honeycomb Plate
508 (Fisher Scientific). The plates were transferred to a Bioscreen C plate reader and incubated for 36
509 h at 37°C with continuous shaking, with OD_{600} measurements taken at 3 h intervals.

510

511 **Pigmentation**

512 To analyze pigment production, strains were cultured as described above to PE phase and
513 then incubated at 37°C for an additional 1-3 days. Next, 0.5 ml samples were centrifuged at

514 16,000 x g for 5 min, 200 µl aliquots of each supernatant were placed in a 96-well plate, and then
515 their absorbance at OD_{550} was quantified on a plate reader. To normalize pigment values to cell
516 density, each cell pellet was resuspended in PBS to its original volume, and then the OD_{600} of
517 100 µl aliquots was quantified on a plate reader. All measurements were performed in duplicate.
518
519 **GFP transcriptional reporter experiments**
520 To analyze activity of the *lpg0279-0277* promoter, strains EH224, EH97 and EH102 which
521 each harbor plasmid p*lpg0279-gfp* were cultured overnight to E phase, and then diluted to an
522 OD_{600} of 0.4-0.8 in either AYET or CDM that lacked L-cysteine, L-serine or L-methionine, as
523 indicated. The AYET and CDM bacterial suspensions were supplemented aseptically with 0.135
524 mg/ml ferric nitrate and/or 2.27 mM, 1.14 mM or 0.7 mM L-cysteine, as indicated. All cultures
525 were then further incubated at 37°C for 10-12 h on an orbital shaker. Measurements were taken
526 at 2-3 h intervals by centrifuging 800 µl aliquots, resuspending the pellet in an equal volume of
527 PBS, and quantifying fluorescence of triplicate 200 µl samples at $485_{EX}/528_{EM}$ on a Biotek plate
528 reader. To normalize all fluorescence readings to cell density, the OD_{600} of a 1/10 dilution of
529 each cell suspension was quantified with a spectrophotometer.
530
531 **PHB measurement by Nile Red staining**
532 To analyze intracellular lipid (PHB) content, 4-6 ml aliquots of E phase cultures were first
533 collected by centrifugation (5 min at 5,000 x g) and the cell pellets resuspended in an equal
534 volume of CDM supplemented with thymidine (0.1 mg/ml), chloramphenicol (25 µg/ml), and
535 IPTG (250 µM), but lacking L-cysteine and L-cystine. Cultures were then incubated for 24 h at
536 37°C on an orbital shaker. PHB content was quantified for the initial E phase cultures and again

following the 24 h incubation using the fluorescent dye Nile Red (Invitrogen) as described (45), with the following modifications. Briefly, aliquots of bacterial cultures were collected by centrifugation and resuspended in an equal volume of deionized water before fixing the cells with 1% (v/v) formaldehyde at room temperature for 30 min. After washing to remove the formaldehyde, cell density was adjusted to OD_{600} 0.5 in 1 ml of deionized water, and the cells were stained by adding 1 µl of a 25 mM Nile Red stock solution suspended in DMSO. The cells were incubated at room temperature in the dark for 1 h, and then 200 µl aliquots were measured in triplicate on a Biotek plate reader at $545_{EX}/600_{EM}$.

Survival assay

To assess long-term survival of *L. pneumophila* in the absence of L-cysteine, cultures prepared as for PHB measurement described above were incubated at 37°C on an orbital shaker for 7 days. At the times indicated, duplicate samples were removed, serially diluted, and plated to enumerate CFUs on CYET.

ACKNOWLEDGEMENTS

This work was supported by the Michigan Predoctoral Genetics Training Program (NIH T32-GM-007544; E.D.H.), a University of Michigan Rackham Graduate Student Research Grant (E.D.H.), and the Endowment for Basic Sciences at the University of Michigan Medical School (M.S.S.).

REFERENCES

1. Declerck P. 2010. Biofilms: the environmental playground of *Legionella pneumophila*. Environ Microbiol 12:557-66.

2. Bruggemann H, Hagman A, Jules M, Sismeiro O, Dillies MA, Gouyette C, Kunst F, Steinert M, Heuner K, Coppee JY, Buchrieser C. 2006. Virulence strategies for infecting phagocytes deduced from the *in vivo* transcriptional program of *Legionella pneumophila*. Cell Microbiol 8:1228-40.
3. Oliva G, Sahr T, Buchrieser C. 2018. The life cycle of *L. pneumophila*: cellular differentiation is linked to virulence and metabolism. Front Cell Infect Microbiol 8:3.
4. Molofsky AB, Swanson MS. 2004. Differentiate to thrive: lessons from the *Legionella pneumophila* life cycle. Mol Microbiol 53:29-40.
5. Garduno RA, Garduno E, Hiltz M, Hoffman PS. 2002. Intracellular growth of *Legionella pneumophila* gives rise to a differentiated form dissimilar to stationary-phase forms. Infect Immun 70:6273-83.
6. Abdelhady H, Garduno RA. 2013. The progeny of *Legionella pneumophila* in human macrophages shows unique developmental traits. FEMS Microbiol Lett 349:99-107.
7. Pine L, George JR, Reeves MW, Harrell WK. 1979. Development of a chemically defined liquid medium for growth of *Legionella pneumophila*. J Clin Microbiol 9:615-26.
8. George JR, Pine L, Reeves MW, Harrell WK. 1980. Amino acid requirements of *Legionella pneumophila*. J Clin Microbiol 11:286-91.
9. Byrne B, Swanson MS. 1998. Expression of *Legionella pneumophila* virulence traits in response to growth conditions. Infect Immun 66:3029-34.
10. Robertson P, Abdelhady H, Garduno RA. 2014. The many forms of a pleomorphic bacterial pathogen-the developmental network of *Legionella pneumophila*. Front Microbiol 5:670.
11. Abbott ZD, Yakhnin H, Babitzke P, Swanson MS. 2015. CsrR, a paralog and direct target of CsrA, promotes *Legionella pneumophila* resilience in water. MBio 6:e00595.
12. Sahr T, Rusniok C, Impens F, Oliva G, Sismeiro O, Coppee JY, Buchrieser C. 2017. The *Legionella pneumophila* genome evolved to accommodate multiple regulatory mechanisms controlled by the CsrA-system. PLoS Genet 13:e1006629.
13. Hammer BK, Swanson MS. 1999. Co-ordination of *Legionella pneumophila* virulence with entry into stationary phase by ppGpp. Mol Microbiol 33:721-31.
14. Hammer BK, Tateda ES, Swanson MS. 2002. A two-component regulator induces the transmission phenotype of stationary-phase *Legionella pneumophila*. Mol Microbiol 44:107-18.
15. Sahr T, Bruggemann H, Jules M, Lomma M, Albert-Weissenberger C, Cazalet C, Buchrieser C. 2009. Two small ncRNAs jointly govern virulence and transmission in *Legionella pneumophila*. Mol Microbiol 72:741-62.
16. Edwards RL, Jules M, Sahr T, Buchrieser C, Swanson MS. 2010. The *Legionella pneumophila* LetA/LetS two-component system exhibits rheostat-like behavior. Infect Immun 78:2571-83.
17. Simm R, Morr M, Kader A, Nimtz M, Romling U. 2004. GGDEF and EAL domains inversely regulate cyclic di-GMP levels and transition from sessility to motility. Mol Microbiol 53:1123-34.
18. Tchigvintsev A, Xu X, Singer A, Chang C, Brown G, Proudfoot M, Cui H, Flick R, Anderson WF, Joachimiak A, Galperin MY, Savchenko A, Yakunin AF. 2010. Structural insight into the mechanism of c-di-GMP hydrolysis by EAL domain phosphodiesterases. J Mol Biol 402:524-38.

19. Tamayo R, Pratt JT, Camilli A. 2007. Roles of cyclic diguanylate in the regulation of bacterial pathogenesis. Annu Rev Microbiol 61:131-148.
20. Levi A, Folcher M, Jenal U, Shuman HA. 2011. Cyclic diguanylate signaling proteins control intracellular growth of *Legionella pneumophila*. MBio 2:e00316-10.
21. Allombert J, Lazzaroni JC, Bailo N, Gilbert C, Charpentier X, Doublet P, Vianney A. 2014. Three antagonistic cyclic di-GMP-catabolizing enzymes promote differential Dot/Icm effector delivery and intracellular survival at the early steps of *Legionella pneumophila* infection. Infect Immun 82:1222-33.
22. Pecastaings S, Allombert J, Lajoie B, Doublet P, Roques C, Vianney A. 2016. New insights into *Legionella pneumophila* biofilm regulation by c-di-GMP signaling. Biofouling 32:935-48.
23. Stock AM, Robinson VL, Goudreau PN. 2000. Two-component signal transduction. Annu Rev Biochem 69:183-215.
24. Zschiedrich CP, Keidel V, Szurmant H. 2016. Molecular mechanisms of two-component signal transduction. J Mol Biol 428:3752-75.
25. Romling U, Galperin MY, Gomelsky M. 2013. Cyclic di-GMP: the first 25 years of a universal bacterial second messenger. Microbiol Mol Biol Rev 77:1-52.
26. Tao J, Li C, Luo C, He C. 2014. RavA/RavR two-component system regulates *Xanthomonas campestris* pathogenesis and c-di-GMP turnover. FEMS Microbiol Lett 358:81-90.
27. Levet-Paulo M, Lazzaroni JC, Gilbert C, Atlan D, Doublet P, Vianney A. 2011. The atypical two-component sensor kinase Lpl0330 from *Legionella pneumophila* controls the bifunctional diguanylate cyclase-phosphodiesterase Lpl0329 to modulate bis-(3'-5')-cyclic dimeric GMP synthesis. J Biol Chem 286:31136-44.
28. Osbourn AE, Field B. 2009. Operons. Cell Mol Life Sci 66:3755-75.
29. Cormack BP, Valdivia RH, Falkow S. 1996. FACS-optimized mutants of the green fluorescent protein (GFP). Gene 173:33-8.
30. Abu-Zant A, Asare R, Graham JE, Abu Kwaik Y. 2006. Role for RpoS but not RelA of *Legionella pneumophila* in modulation of phagosome biogenesis and adaptation to the phagosomal microenvironment. Infect Immun 74:3021-6.
31. Rasis M, Segal G. 2009. The LetA-RsmYZ-CsrA regulatory cascade, together with RpoS and PmrA, post-transcriptionally regulates stationary phase activation of *Legionella pneumophila* Icm/Dot effectors. Mol Microbiol 72:995-1010.
32. Albert-Weissenberger C, Sahr T, Sismeiro O, Hacker J, Heuner K, Buchrieser C. 2010. Control of flagellar gene regulation in *Legionella pneumophila* and its relation to growth phase. J Bacteriol 192:446-55.
33. Appelt S, Heuner K. 2017. The flagellar regulon of *Legionella*-a review. Front Cell Infect Microbiol 7:454.
34. Bachman MA, Swanson MS. 2001. RpoS co-operates with other factors to induce *Legionella pneumophila* virulence in the stationary phase. Mol Microbiol 40:1201-14.
35. Lange R, Hengge-Aronis R. 1991. Identification of a central regulator of stationary-phase gene expression in *Escherichia coli*. Mol Microbiol 5:49-59.
36. Chiang SM, Schellhorn HE. 2010. Evolution of the RpoS regulon: origin of RpoS and the conservation of RpoS-dependent regulation in bacteria. J Mol Evol 70:557-71.
37. Dong T, Schellhorn HE. 2010. Role of RpoS in virulence of pathogens. Infect Immun 78:887-97.

653 38. Warren WJ, Miller RD. 1979. Growth of Legionnaires disease bacterium (*Legionella*
654 *pneumophila*) in chemically defined medium. J Clin Microbiol 10:50-5.
655 39. Ewann F, Hoffman PS. 2006. Cysteine metabolism in *Legionella pneumophila*:
656 characterization of an L-cystine-utilizing mutant. Appl Environ Microbiol 72:3993-4000.
657 40. Zusman T, Gal-Mor O, Segal G. 2002. Characterization of a *Legionella pneumophila*
658 *relA* insertion mutant and roles of RelA and RpoS in virulence gene expression. J
659 Bacteriol 184:67-75.
660 41. Bachman MA, Swanson MS. 2004. The LetE protein enhances expression of multiple
661 LetA/LetS-dependent transmission traits by *Legionella pneumophila*. Infect Immun
662 72:3284-93.
663 42. Steinert M, Engelhard H, Flugel M, Wintermeyer E, Hacker J. 1995. The Lly protein
664 protects *Legionella pneumophila* from light but does not directly influence its
665 intracellular survival in Hartmannella-vermiformis. Appl Environ Microbiol 61:2428-
666 2430.
667 43. Chatfield CH, Cianciotto NP. 2007. The secreted pyomelanin pigment of *Legionella*
668 *pneumophila* confers ferric reductase activity. Infect Immun 75:4062-70.
669 44. Gillmaier N, Schunder E, Kutzner E, Tlapak H, Rydzewski K, Herrmann V, Stammler M,
670 Lasch P, Eisenreich W, Heuner K. 2016. Growth-related metabolism of the carbon
671 storage poly-3-hydroxybutyrate in *Legionella pneumophila*. J Biol Chem 291:6471-82.
672 45. James BW, Mauchline WS, Dennis PJ, Keevil CW, Wait R. 1999. Poly-3-
673 hydroxybutyrate in *Legionella pneumophila*, an energy source for survival in low-
674 nutrient environments. Appl Environ Microbiol 65:822-7.
675 46. Greenspan P. 1985. Nile red: a selective fluorescent stain for intracellular lipid droplets.
676 Cell Bio 100:965-973.
677 47. Edwards RL, Dalebroux ZD, Swanson MS. 2009. *Legionella pneumophila* couples fatty
678 acid flux to microbial differentiation and virulence. Mol Microbiol 71:1190-1204.
679 48. Trigui H, Dudyk P, Oh J, Hong JI, Faucher SP. 2015. A regulatory feedback loop
680 between RpoS and SpoT supports the survival of *Legionella pneumophila* in water. Appl
681 Environ Microbiol 81:918-28.
682 49. Skaliy P, McEachern HV. 1979. Survival of the Legionnaires' disease bacterium in water.
683 Ann Intern Med 90:662-3.
684 50. Paszko-Kolva C, Shahamat M, Colwell RR. 1992. Long-term survival of *Legionella*
685 *pneumophila* serogroup 1 under low-nutrient conditions and associated morphological
686 changes. FEMS Microbiol Ecol 11:45-55.
687 51. Mendis N, McBride P, Faucher SP. 2015. Short-term and long-term survival and
688 virulence of *Legionella pneumophila* in the defined freshwater medium Fraquil. PLoS
689 One 10:e0139277.
690 52. Li L, Mendis N, Trigui H, Faucher SP. 2015. Transcriptomic changes of *Legionella*
691 *pneumophila* in water. BMC Genomics 16:637.
692 53. Duerig A, Abel S, Folcher M, Nicollier M, Schwede T, Amiot N, Giese B, Jenal U. 2009.
693 Second messenger-mediated spatiotemporal control of protein degradation regulates
694 bacterial cell cycle progression. Genes Dev 23:93-104.
695 54. He M, Zhang JJ, Ye M, Lou Y, Yang XF. 2014. Cyclic di-GMP receptor PlzA controls
696 virulence gene expression through RpoS in *Borrelia burgdorferi*. Infect Immun 82:445-
697 52.

55. Conner JG, Zamorano-Sanchez D, Park JH, Sondermann H, Yildiz FH. 2017. The ins and outs of cyclic di-GMP signaling in *Vibrio cholerae*. Curr Opin Microbiol 36:20-29.
56. Borziak K, Zhulin IB. 2007. FIST: a sensory domain for diverse signal transduction pathways in prokaryotes and ubiquitin signaling in eukaryotes. Bioinformatics 23:2518-21.
57. Hossain S, Boon EM. 2017. Discovery of a novel nitric oxide binding protein and nitric-oxide-responsive signaling pathway in *Pseudomonas aeruginosa*. ACS Infect Dis 3:454-461.
58. Carlson HK, Vance RE, Marletta MA. 2010. H-NOX regulation of c-di-GMP metabolism and biofilm formation in *Legionella pneumophila*. Mol Microbiol 77:930-42.
59. Rao C, Benhabib H, Ensminger AW. 2013. Phylogenetic reconstruction of the *Legionella pneumophila* Philadelphia-1 laboratory strains through comparative genomics. PLoS One 8:e64129.
60. Bryan A, Abbott ZD, Swanson MS. 2013. Constructing unmarked gene deletions in *Legionella pneumophila*. Methods Mol Biol 954:197-212.
61. Bryan A, Harada K, Swanson MS. 2011. Efficient generation of unmarked deletions in *Legionella pneumophila*. Appl Environ Microbiol 77:2545-8.
62. Yu D, Ellis HM, Lee EC, Jenkins NA, Copeland NG, Court DL. 2000. An efficient recombination system for chromosome engineering in *Escherichia coli*. Proc Natl Acad Sci U S A 97:5978-83.
63. Berger KH, Isberg RR. 1993. Two distinct defects in intracellular growth complemented by a single genetic locus in *Legionella pneumophila*. Mol Microbiol 7:7-19.
64. Dalebroux ZD, Edwards RL, Swanson MS. 2009. SpoT governs *Legionella pneumophila* differentiation in host macrophages. Mol Microbiol 71:640-58.
65. Molofsky AB, Swanson MS. 2003. *Legionella pneumophila* CsrA is a pivotal repressor of transmission traits and activator of replication. Mol Microbiol 50:445-61.
66. Datsenko KA, Wanner BL. 2000. One-step inactivation of chromosomal genes in *Escherichia coli* K-12 using PCR products. Proc Natl Acad Sci U S A 97:6640-5.

FIGURES

Figure 1

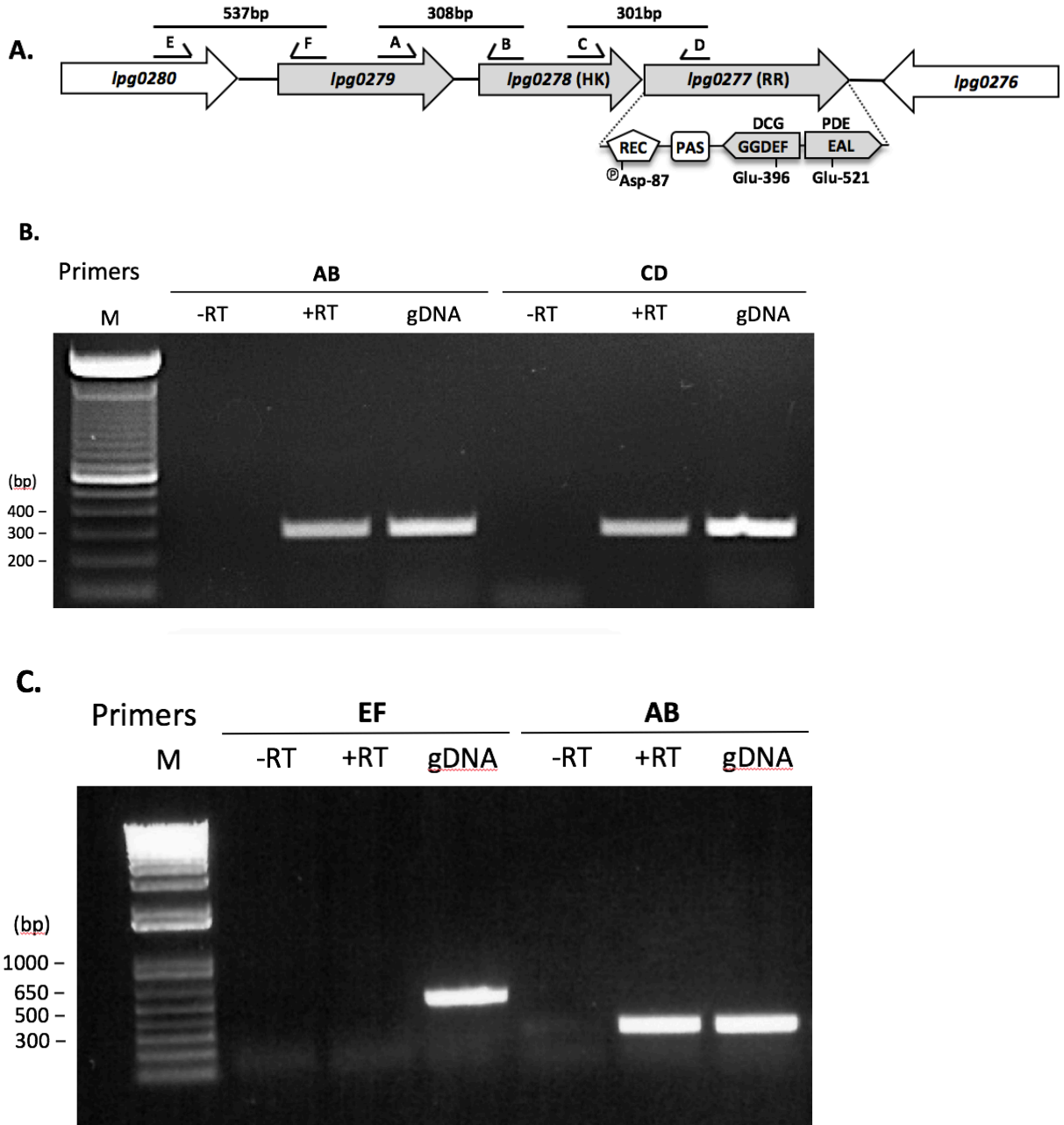

Fig. 1. The genes *lpg0279*, *lpg0278* and *lpg0277* constitute an operon. (A) Schematic of the locus containing *lpg0279*, the TCS-encoding genes *lpg0278* and *lpg0277*, and the primer sets used to characterize mRNA by PCR. Also shown are the genes located 5' and 3' of the *lpg0279-2077* locus. Co-transcription of **(B)** *lpg0279, lpg0278* and *lpg0277* and **(C)** *lpg0280* and *lpg0279* and, as a positive control, *lpg0279* and *lpg0278* was assessed by end-point PCR assay with or without reverse transcriptase **(RT)** using RNA isolated from PE phase WT *L. pneumophila* that was converted to cDNA. As a reference for the PCR product length expected for each primer pair, genomic DNA **(gDNA)** was also used as a template. **M:** DNA size marker.

742 **Figure 2**
743

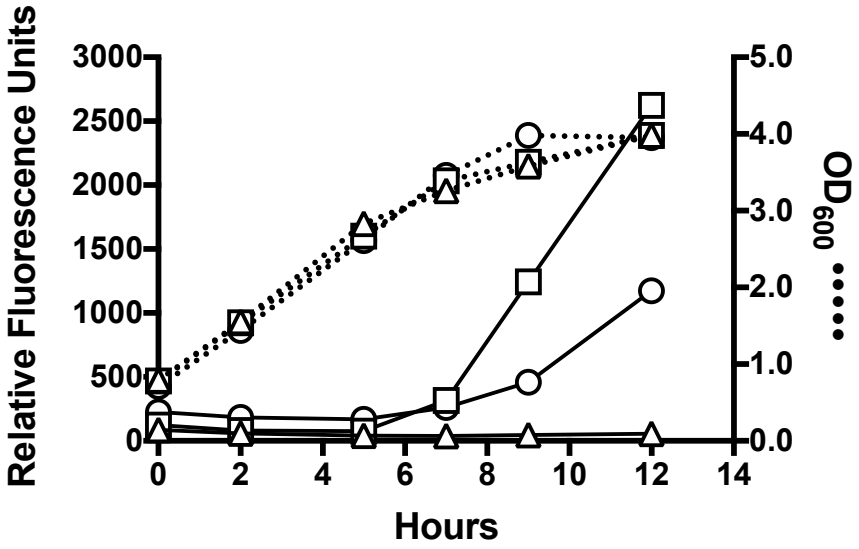

744
745
746 **Fig. 2. Promoter activity for the *lpg0279-77* operon increases upon entry into PE phase.** GFP fluorescence
747 generated by the transcriptional reporter p*lpg0279-gfp* (○). Negative control strain is Lp02 carrying the empty
748 pBH6119 vector (Δ); PE reference strain carries the flagellin subunit reporter p*flaA-gfp* (□). For all strains,
749 overnight E phase cultures were diluted to a starting OD_{600} of 0.8, incubated at 37°C, and then their fluorescence
750 was measured at 2-3 h intervals. Relative Fluorescence Units (solid lines) was calculated as Fluorescence
751 Units/OD_{600} (dotted lines) and represent the means ± SE of triplicate samples. In each case, error < 5%. Data shown
752 are representative of results obtained in at least three independent experiments.
753
754

Figure 3

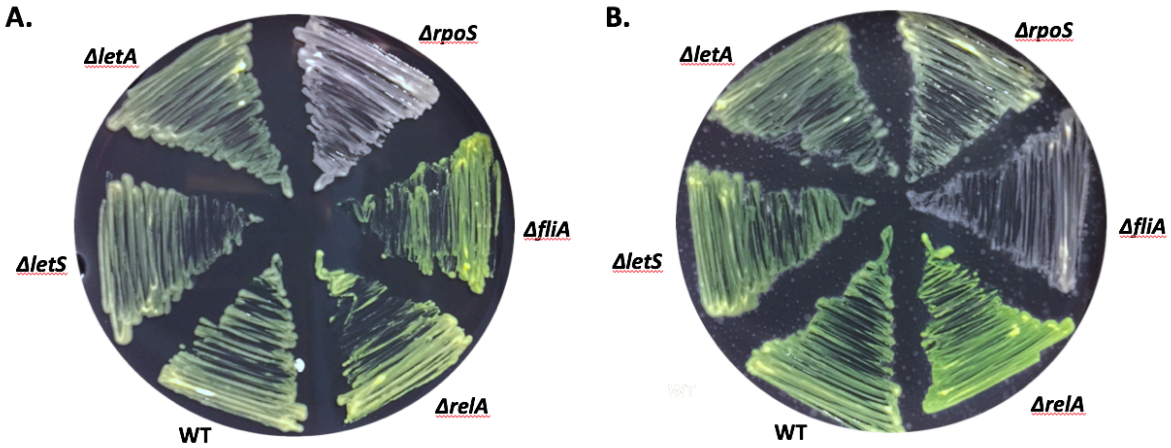

Fig. 3. Expression of *lpg0279-77* is RpoS-dependent. Images obtained in ambient light of WT Lp02 and *letA*, *letS*, *relA*, *rpoS* and *fliA* mutants harboring the transcriptional reporter plasmids **(A)** p*lpg0279-gfp* or **(B)** p*flaA-gfp*, which serves as a reference for PE phase gene expression. The strains indicated were cultured on CYET at 37°C for 3 days to allow for bacterial growth and GFP accumulation.

766 **Figure 4**

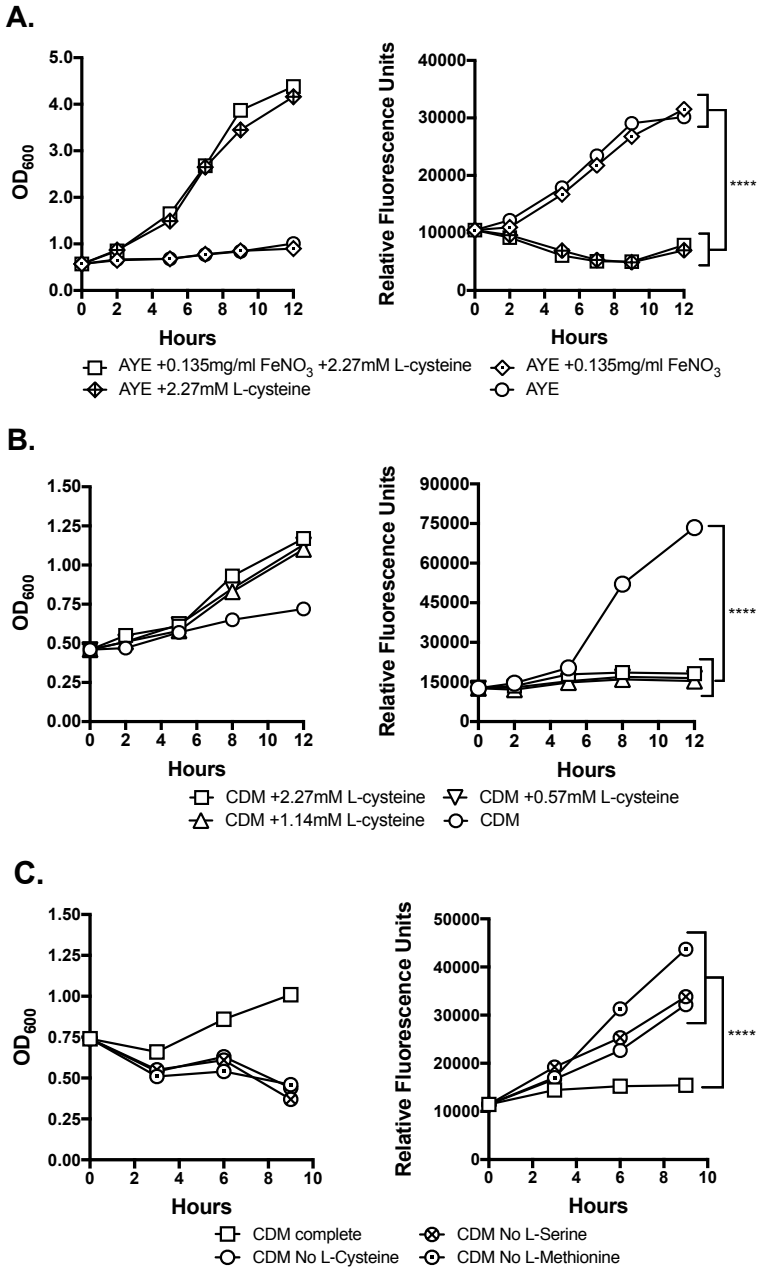

767

768

769

770

771 **Fig. 4. Nutrient limitation induces expression of *lpg0279-77*.** To examine the impact of nutrient limitation on
772 *lpg0279-77* transcription, E phase Lp02 cultures carrying the p*lpg0279-gfp* reporter plasmid were exposed to culture
773 conditions shown and incubated for 9-12 h at 37°C on an orbital shaker, with GFP fluorescence and cell density
774 (OD_{600}) measured at 2-3 h intervals. **(A)** OD_{600} measurements and RFU values obtained for cultures exposed to AYE
775 medium with or without 0.135 mg/ml ferric nitrate and/or 2.27 mM L-cysteine. **(B)** OD_{600} measurements and RFU
776 values obtained for cultures exposed to CDM without or with the indicated concentration of L-cysteine. **(C)** OD_{600}
777 and RFU values obtained for cultures exposed to CDM with or without either L-cysteine, L-methione, or L-serine.
778 RFU symbols represent the means ± SE of triplicate GFP fluorescence readings, normalized to OD_{600} values
779 obtained by measuring a 1/10 dilution of cell culture in a spectrophotomer (short error bars are masked by symbols).
780 A two-tailed Student's *t*-test was used to determine statistically significant differences between groups at 12 h (****,
781 $p < 0.0001$). Data shown are representative of results obtained in two or more independent experiments.

Figure 5

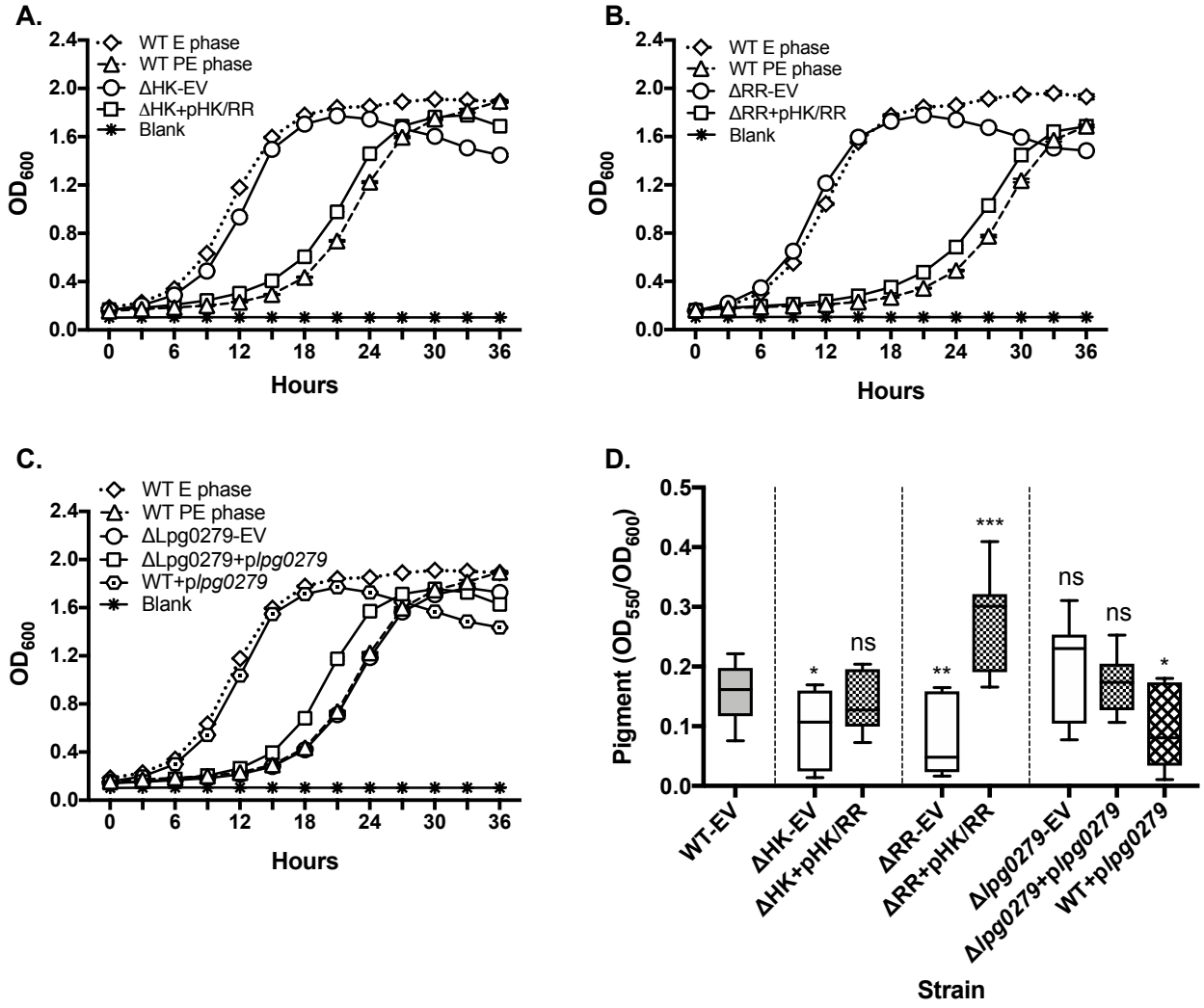

Fig. 5. *L. pneumophila* lacking a complete TCS or ectopically expressing *lpg0279* resemble WT E phase cells.

The growth kinetics of WT *L. pneumophila* inocula in E phase (dotted lines) or PE phase (dashed lines) was compared to PE phase inocula of **(A)** an ΔHK mutant and its complement, **(B)** an ΔRR mutant and its complement, and **(C)** an Δ*lpg0279* mutant and its complement, together with a WT strain of *L. pneumophila* constitutively expressing *lpg0279*. With the exception of the WT E phase reference culture (OD_{600} < 2.0), all strains were cultured overnight in AYET medium to OD_{600} > 3.5 (corresponding to WT PE phase cultures), then diluted to a starting OD_{600} of ~0.1 and incubated for 36 h in a Bioscreen growth curve analyzer set at 37°C with continuous shaking; OD_{600} measurements were obtained at 3 h intervals. Shown are means ± SE of triplicate samples, and data shown are representative of three independent experiments. (**D**) Pigment accumulation in late PE phase cultures of ΔHK, ΔRR and Δ*lpg0279* mutants and the corresponding complemented strains, and of WT *L. pneumophila* constitutively expressing *lpg0279*. Supernatants of broth cultures maintained in PE phase for 1 or 3 days were collected by centrifugation, their absorbance at OD_{550} quantified and then normalized to cell density (OD_{600}). Results shown are the means ± SE of pooled data from three independent experiments, with duplicate readings obtained for each measurement. A two-tailed Student's *t*-test was used to determine statistically significant differences in pigmentation compared to WT-EV (**ns**: not significant; *, p <0.05; **, p < 0.01; ***, p < 0.001). **EV:** strain harbors the pMMB206cam empty vector.

Figure 6

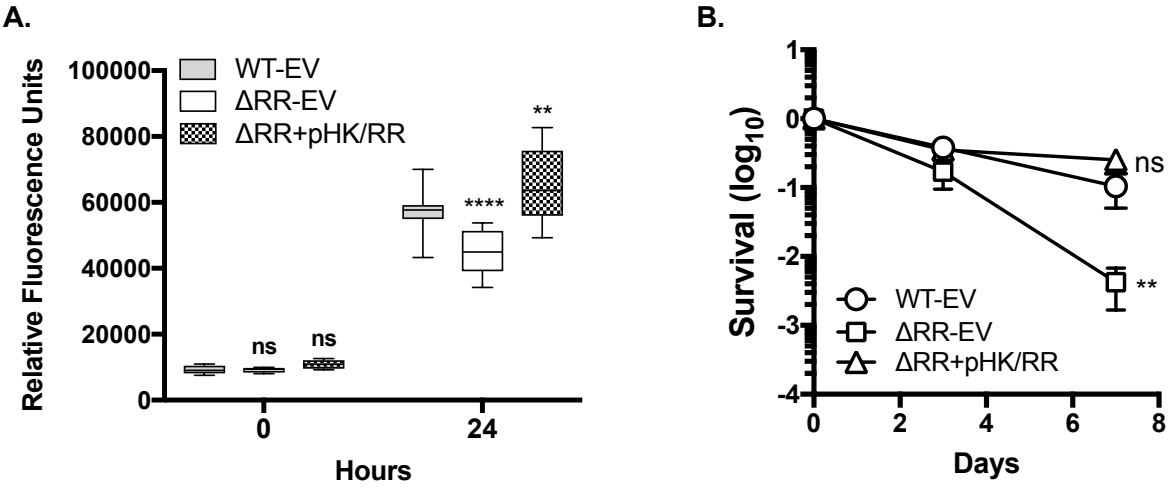

Fig. 6. The TCS promotes PHB production and long-term viability. E phase cultures of WT *L. pneumophila*, the ΔRR mutant, and the ΔRR complemented strain harboring pHK/RR were collected by centrifugation, resuspended in CDM lacking L-cysteine, and incubated at 37°C on an orbital shaker for up to 7 d. **(A)** Quantification of PHB content before and after 24 h CDM exposure. Results shown are the means ± SE of pooled data obtained from triplicate samples in four independent experiments. A two-tailed Student's *t*-test was used to determine statistically significant differences in fluorescence compared to WT-EV (**ns**: no significance; **, $p < 0.01$; ****, $p < 0.0001$). **(B)** Survival was quantified by plating serial dilutions of the cultures indicated and enumerating CFUs before (titer) and after 3 and 7 d incubation. Shown are ratio of CFU(day)/CFU(titer), with symbols representing the means ± SE of pooled data obtained from duplicate samples in four independent experiments. The Mann-Whitney test was used to determine statistically significant differences in survival compared to WT-EV (**ns**: no significance; **, $p < 0.01$). **EV:** strain harbors the pMMB206cam empty vector.

Figure 7

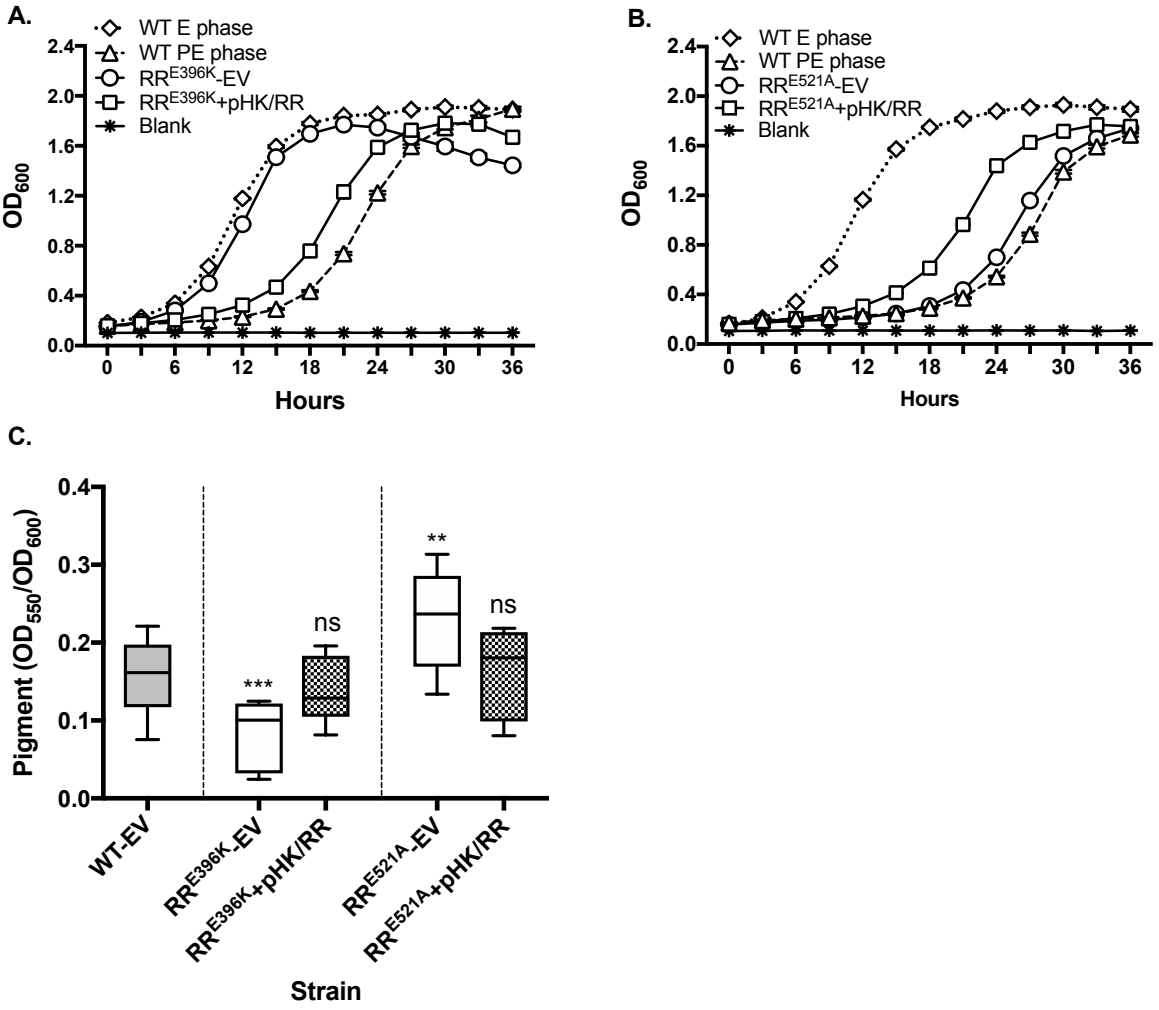

Fig. 7. The DCG activity of RR Lpg0277 promotes transition to PE phase.
Growth kinetics in AYET of WT *L. pneumophila* inocula in E (dotted lines) or PE phase (dashed lines) was compared to PE phase inocula of **(A)** RR^{E396K} point mutant and **(B)** RR^{E521A} point mutant strains. Symbols denote the means ± SE of triplicate samples (short error bars are masked by symbols), and data are representative of three independent experiments. **(C)** Pigment accumulation by WT *L. pneumophila* after maintenance in PE phase for 1-3 days, compared with the RR^{E396K} DGC and RR^{E521A} PDE point mutants and their respective complemented strains. Results shown are the means ± SE of pooled data obtained from duplicate samples in three independent experiments. A two-tailed Student's *t*-test was used to determine statistically significant differences in pigmentation compared to WT (**ns**: not significant; $^{**}p < 0.01$; ***, $p < 0.001$). **EV:** strain harbors the pMMB206cam empty vector.

Figure 8

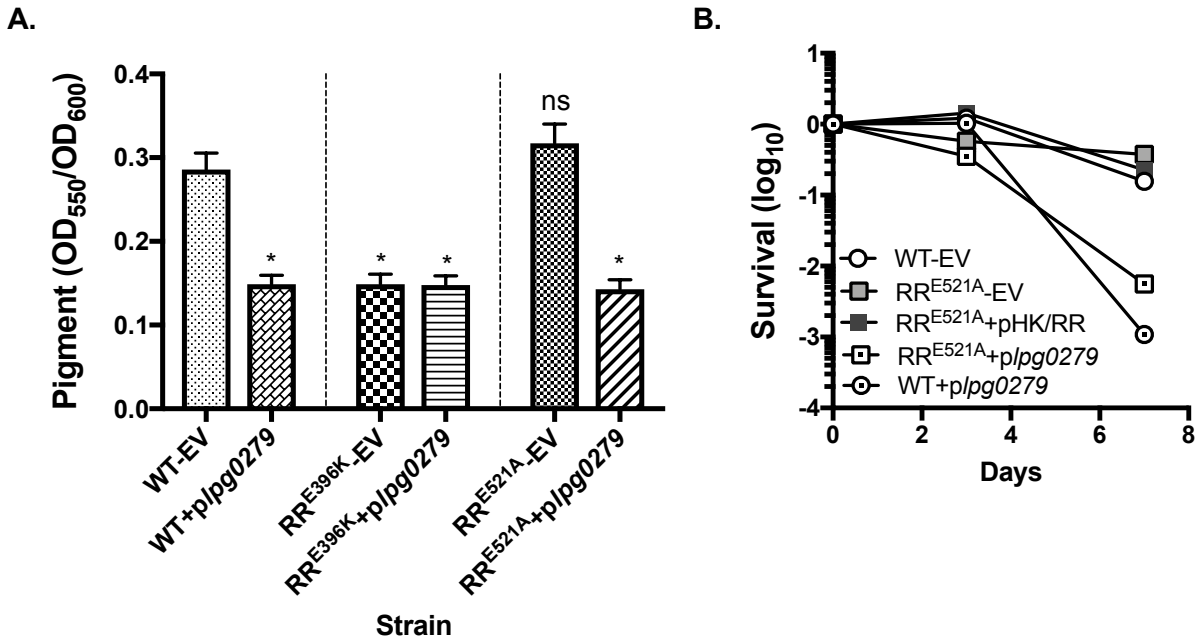

Fig. 8. Constitutively expressed *lpg0279* is epistatic to RR^{E521A} PDE mutation.
(A) Pigment accumulation by PE phase WT *L. pneumophila* and the Lpg0277 RR^{E396K} CDG and RR^{E521A} PDE point mutants that do or do not constitutively express p*lpg0279*. Shown are the means ± SE of four samples and are representative of results obtained in one other independent experiment. The Mann-Whitney test was used to determine statistically significant differences in pigmentation compared to WT (**ns**: not significant; *, p <0.05). **(B)** Survival of WT *L. pneumophila* and the RR^{E521A} PDE mutant that do or do not constitutively express p*lpg0279* or the complementing pHK/RR plasmid. All strains were cultured in AYE to E phase, resuspended in CDM without L-cystine, and incubated at 37°C on an orbital shaker for up to 7 days. At the times shown, culture aliquots were serially diluted for CFU enumeration on CYET. Symbols shown are the ratio of CFU(day)/CFU(titer) of duplicate samples, and data is representative of results obtained in three independent experiments. **EV:** strain harbors the pMMB206cam empty vector.

852 **Figure 9**
853

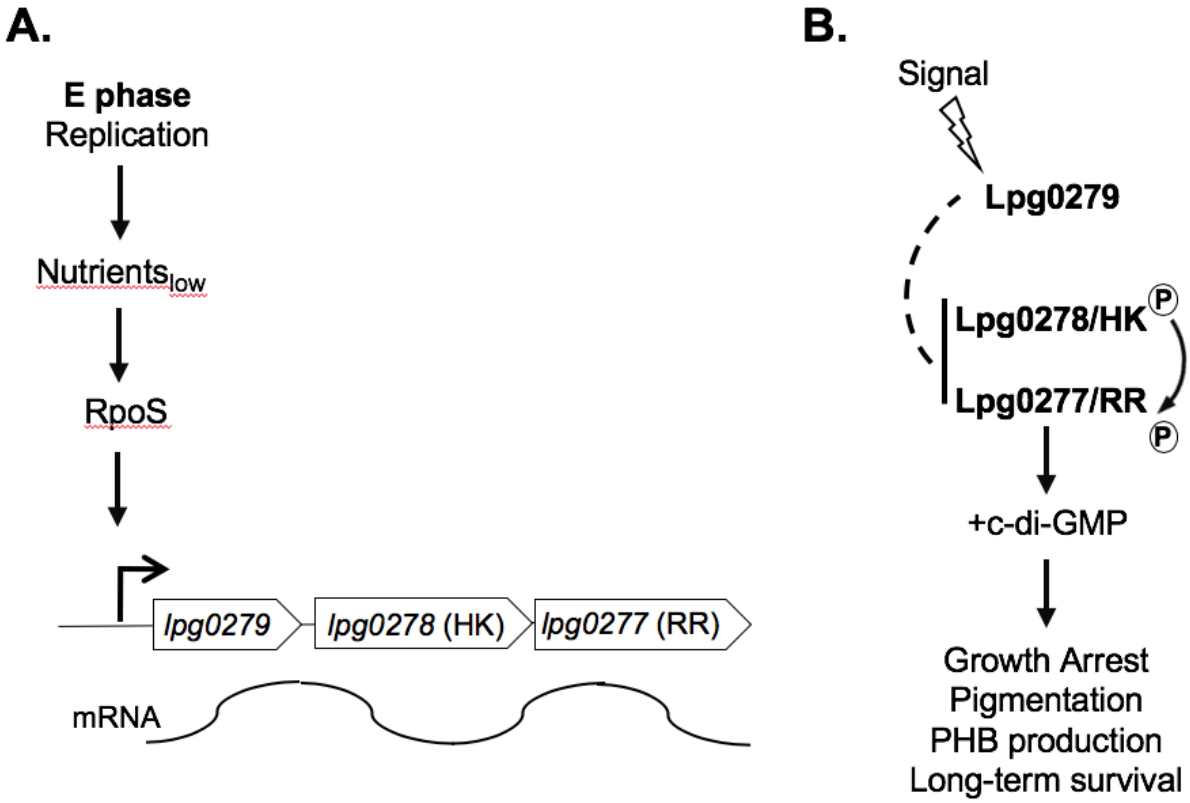

854
855
856 **Fig. 9. Model for *lpg0279-77* regulation of *L. pneumophila* differentiation.** **(A)** When amino acids become
857 limiting, RpoS equips replicating *L. pneumophila* to induce transcription of the *lpg0279-0277* operon which encodes
858 a putative repressor and a Two Component System. **(B)** Initially Lpg0279 suppresses signaling by the
859 Lpg0278/0277 TCS. In response to prolonged environmental stress, the TCS is derepressed and HK Lpg0278
860 phosphorylates RR Lpg0277. The DCG domain of RR Lpg0277 generates c-di-GMP, which arrests *L. pneumophila*
861 replication, triggers production of pigment and PHB storage granules, and promotes survival in nutrient-poor
862 environments.
863
864

SUPPLEMENTAL TABLES

Table S1. Strains used in this study

Strain	Relevant properties	Source
E. coli		
DH5α	*supE44 ΔlacU169 (*80 *lacZΔM15) hsdR17 recA1 endA1 gyrA96 thi-1 relA1*	Laboratory collection
DY330	W3110 Δ*lacU169 gal490 λcI857* Δ(*cro-bioA*)	(62)
EH207	DH5α p*lpg0279-gfp*	This work
EH272	DH5α p*lpg0279-77*	This work
EH140	DH5α p*lpg0279*	This work
L. pneumophila	**Relevant properties**	**Source**
MB110	Lp02 wild type; *thyA hsdR rpsL* (Str^r)	(63)
EH284	Lp02 pMMB206cam	This work
EH286	Lp02 Δ*lpg0277*::*FRT* pMMB206cam	This work
EH276	Lp02 Δ*lpg0277*::*FRT* p*lpg0278-77*	This work
EH357	Lp02 Δ*lpg0278*::*FRT* pMMB206cam	This work
EH352	Lp02 Δ*lpg0278*::*FRT* p*lpg0278-77*	This work
EH350	Lp02 Δ*lpg0279*::*FRT-kan-FRT* pMMB206cam	This work
EH160	Lp02 Δ*lpg0279*::*FRT-kan-FRT* p*lpg0279*	This work
EH151	Lp02 p*lpg0279*	This work
EH344	Lp02 $Lpg0277^{E396K}$ pMMB206cam	This work
EH311	Lp02 $Lpg0277^{E396K}$ p*lpg0278-77*	This work
EH346	Lp02 $Lpg0277^{E521A}$ pMMB206cam	This work
EH314	Lp02 $Lpg0277^{E521A}$ p*lpg0278-77*	This work
EH102	Lp02 p*flaA-gfp*	This work
EH224	Lp02 p*lpg0279-gfp*	This work
EH97	Lp02 pBH6119	This work
MB410	Lp02 Δ*fliA::kan*	(14)
MB443	Lp02 Δ*rpoS::kan*	(34)
MB696	Lp02 Δ*relA::kan*	(64)
MB413	Lp02 Δ*letA::kan*	(14)
MB416	Lp02 Δ*letS::kan*	(14)
EH358	Lp02 Δ*fliA* p*lpg0279-gfp*	This work
EH360	Lp02 Δ*rpoS* p*lpg0279-gfp*	This work
EH366	Lp02 Δ*relA* p*lpg0279-gfp*	This work
EH362	Lp02 Δ*letA* p*lpg0279-gfp*	This work
EH364	Lp02 Δ*letS* p*lpg0279-gfp*	This work
MB1230	Lp02 Δ*letA::kan* p*flaA-gfp*	(14)
EH370	Lp02 Δ*letS::kan* p*flaA-gfp*	This work
MB1234	Lp02 Δ*rpoS::kan* p*flaA-gfp*	(34)
MB1014	Lp02 Δ*relA::kan* p*flaA-gfp*	(64)
EH368	Lp02 Δ*fliA::kan* p*flaA-gfp*	This work
EH373	Lp02 $Lpg0277^{E521A}$ p*lpg0279*	This work
EH375	Lp02 $Lpg0277^{E396K}$ p*lpg0279*	This work

871 **Table S2. Primers and plasmids used in this study**
872
873 Restriction enzyme sequences in **bold**

Primers		
Construction of *lpg0279-gfp*		
EH21	AAA**GGATCC**AAATATGGTTCACACCCTGAAAAACTCGCAAC	Amplify 5' of *lpg0279* adding BamHI and XbaI
EH43	AAA**TCTAGA**ATTGCTGTGACTTGGAGGGAGCGGATGATTAATTATAG	
Construction of complementing vector p*lpg0278-77*		
EH69	TATA**GGATCC**ATGACAGAAATGCATCGGTTGTTGC	Amplify *lpg0278-lpg0277* adding BamHI and HindIII
EH70	AAAT**AAGCTT**TTATTTTGTCCTATTTCCTTGCAGAAGTTTTTC	
Construction of vector p*lpg0279* (optimal RBS in *italics*)		
79OE-F	AAA**GGATCC***GAAGGAGATATACAT*TCACAGCAATATGATGAAAATTGAATCATTTC	Amplify *lpg0279* adding BamHI and HindIII
79OE-R	AAA**AAGCTT**CTTTTTGGTTTATGGACTCTCTAACAGGGTCG	
Construction of deletion mutants (PO and P2 oligos from pKD4 underlined)		
77del-F	ACTGTCCGCTATAAAAACCATGCTTGACGAAAAC	Amplify *lpg0277* + ~700bp flanking DNA
77del-R	AAGAGAGTATGAAGAACTTGTTACAACGCATGGTGG	
77PO-F	TTTGCCCATCAATCCCAAAACCTTGAGTACGAGGTAGAATGTGTAGGCTGGAGCTGCTTC	Amplify Kan cassette with homology to *lpg0277*
77P2-R	CGGATAGCTCTTATAGATGCCAATGCGATTTTTATCCATATGAATATCCTCCTTAGTTCC	
78del-F	GAAAAATTGTAGACCATTGCATTGGGGCAGTAGG	Amplify *lpg0278* + ~700bp flanking DNA
78del-R	TTGAGTAATTGCCTTGACATATACTGAATGAGTTGGG	
78PO-F	TAGAGAGTCCATAAACCAAAAAGGAATTCAGTAATAATGTGTGTAGGCTGGAGCTGCTTC	Amplify Kan cassette with homology to *lpg0278*
78PO-R	AAAGATTCAGTACTCATTTCTACCTCGTACTCAAGGCATATGAATATCCTCCTTAGTTCC	
79del-F	AATACTTAAAGGAAACCCATCCGACCATTCAAGC	Amplify *lpg0279* + ~700bp flanking DNA
79del-R	GTTTTCGTCAAGCATGGTTTTTATAGCGGACAG	
79PO-F	ACTATAATTAATCATAAGATAAATCCAAGTCACAGCAATTGTGTAGGCTGGAGCTGCTTC	Amplify Kan cassette with homology to *lpg0279*
79PO-R	TGCATTTCTGTCATTATTACTGAATTCCTTTTTGGTCATATGAATATCCTCCTTAGTTCC	
Construction of point mutants		
E396K-F	AAAGCATTACAAACTTATCCCCACCAAGTCTGGCG	
E396K-R	CGCCAGACTTGGTGGGGATAAGTTTGTAATGCTTT	
E521A-F	TCCACCGGATTAATGCTGCCATGGAACGAATCTCA	
E521A-R	TGAGATTCGTTCCATGGCAGCATTAATCCGGTGGA	
D87N-F	GGGGCATTCTTATGTTAACAAAAGCGAGTGGGTATG	
D87N-R	CATACCCACTCGCTTTTGTTAACATAAGAATGCCCC	
Other oligos		
EH13	TCGGCAGAAGATTGGTATTAGG	Fig 1A, set A/B
EH14	GCAATAAATTGAGTCCAACTCTCC	

EH1	GGATCTGGGTGGTACACTTTATG	Fig 1A, set C/D
EH2	CAATGCCTTGAGTCGCTACA	
EH55	TGAGTACTATCGATGCCATAAAATCTCT	Fig 1A, set E/F
EH56	AGGCTTGAGCCAATTCTTCAATT	

874
875

Plasmids		
pGEMT-easy	Cloning vector; Amp^R	Promega
pMMB206cam	Broad host range vector; pMMB66EH derivative; Cam^R	(65)
pKD4	Source of *FRT-kan-FRT* allele	(66)
pBH6119	~800 bp XbaI/PstI fragment (containing GFP gene from p*GFPmut3*) inserted into pJB98 at XbaI and PstI sites; Amp^R; tdΔi	(13)
p*flaA-gfp*	pBH6119 with ~300 bp of *flaA* promoter region cloned into *Bam*HI and *Xba*I sites; GFP transcriptional reporter plasmid	This work
p*lpg0279-gfp*	pBH6119 with ~830 bp of the *lpg0279-77* promoter region cloned into *Bam*HI and *Xba*I sites; GFP transcriptional reporter plasmid	This work
pHK/RR	pMMB206cam with ~3.6 kb PCR product of the *lpg0278* through *lpg0277* ORFs cloned into *Bam*HI and *Hind*II sites; IPTG-inducible plasmid; Cam^R	This work
p*lpg0279*	pMMB206cam with ~1.2 kb PCR product containing the *lpg0279* ORF and optimal RBS cloned into *Bam*HI and *Hind*II sites; IPTG-inducible plasmid; Cam^R	This work

876
877
878

SUPPLEMENTAL FIGURES

Supplemental Figure 1

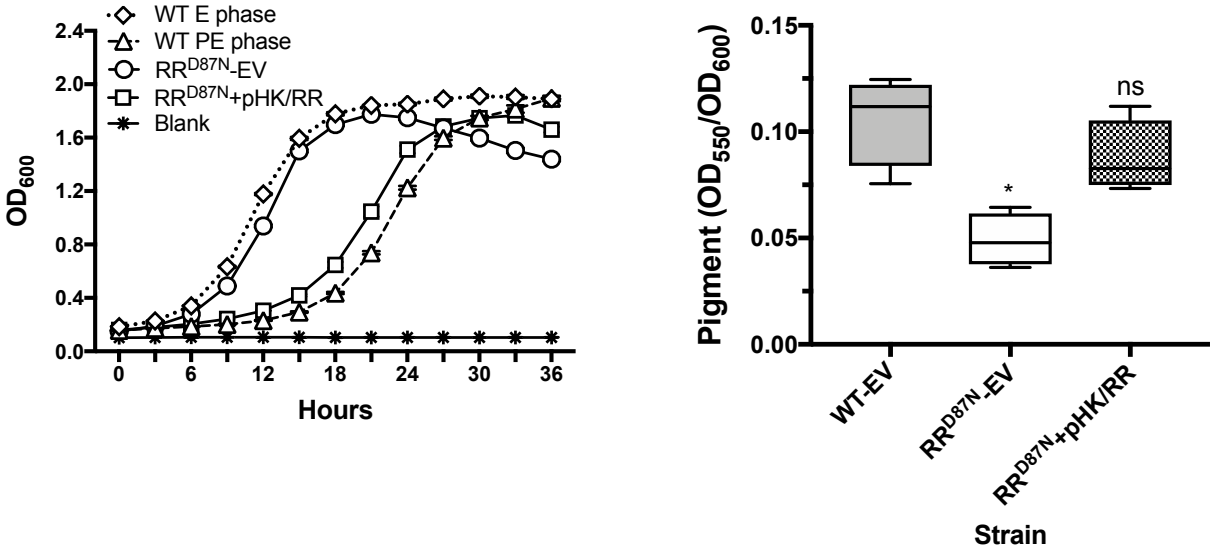

Fig S1. The Lpg0277 RR phosphoacceptor site promotes *L. pneumophila* differentiation to the PE phase. Growth kinetics and pigment production by WT *L. pneumophila* and RR^{D87N} phosphoacceptor site point mutant and the corresponding complemented strain. Results shown are representative of one other independent experiment. The Mann-Whitney test was used to determine statistically significant differences in pigmentation compared to WT (**ns**: not significant; *, p <0.05). **EV:** strain harbors the pMMB206cam empty vector.

Supplemental Figure 2

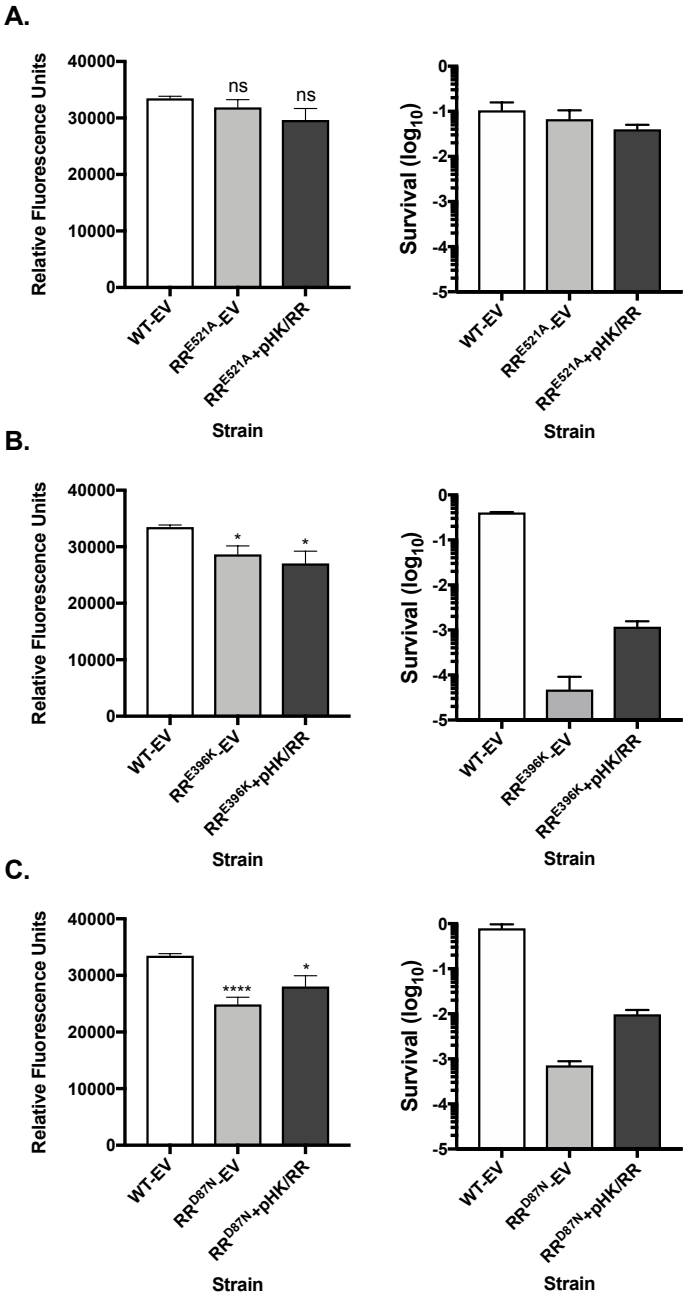

Fig. S2. The GGDEF domain and phosphoacceptor site of the RR contribute to PHB production and promote survival during prolonged nutrient deprivation.
PHB quantification and survival of E phase cultures after 24 h and 7 d L-cysteine deprivation, respectively. WT *L. pneumophila* were compared to (A) RR^{E521A} PDE, (B) RR^{E396K} DCG, and (C) RR^{D87N} phosphoacceptor site point mutants, and the respective complemented strains bearing plasmid pHK/RR. PHB values represent the means ± SE of pooled Nile Red fluorescence data from triplicate samples in four independent experiments. A two-tailed Student's t-test was used to determine statistically significant differences in fluorescence compared to WT-EV (**ns**: no significance; *, $p < 0.05$; ****, $p < 0.0001$). Survival data is the ratio of CFU(day 7)/CFU(titer), and data is representative of results obtained in two or more independent experiments. **EV**: strain harbors the pMMB206cam empty vector.

Supplemental Figure 3

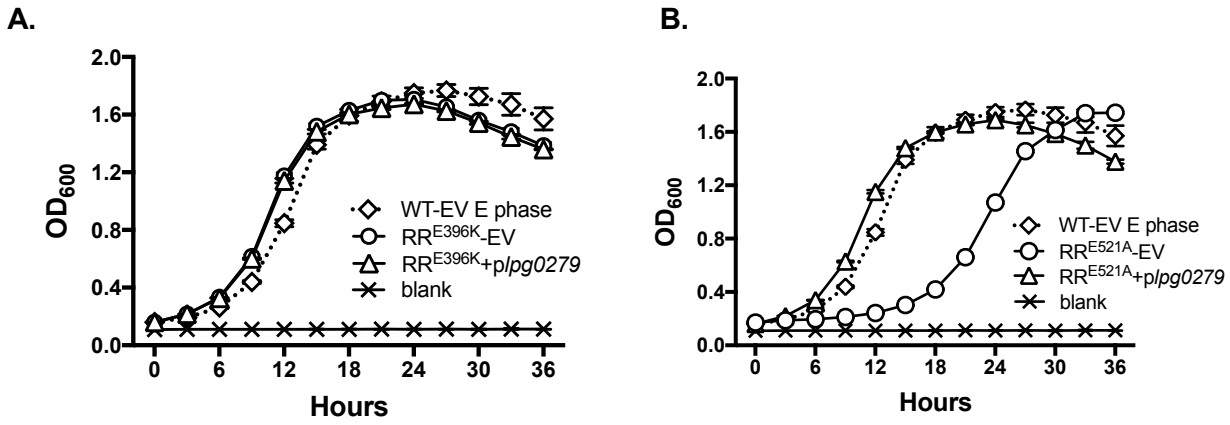

Fig. S3. Disruption of the Lpg0277 RR^{E521A} PDE domain is not sufficient to suppress the differentiation defect of PE phase *L. pneumophila* constitutively expressing *lpg0279*. Growth kinetics of PE phase WT *L. pneumophila* and the **(A)** Lpg0277 RR^{E396K} DCG and **(B)** RR^{E521A} PDE point mutants that harbor either p*lpg0279* or pMMB206 empty vector (**EV**). Symbols denote the means ± SE of triplicate samples, and data shown are representative of one additional independent experiment.